Design and Construction of an Integrated Solar Lighting Pedestrian Crosswalk(s) and Sidewalks with Enhanced Visibility

Master Agreement #: BDV31-977-78

February 2020

Final Report

Disclaimer

The opinions, findings, and conclusions expressed in this publication are those of the authors and not necessarily those of the State of Florida Department of Transportation.

Technical Report Documentation Page

1. Report No.	2. Government Accession No.	3. Recipient's Catalog No.
4. Title and Subtitle *Design and Construction of an Integrated Solar Lighting Pedestrian Crosswalk(s) and Sidewalks with Enhanced Visibility*		5. Report Date *2/2020* 6. Performing Organization Code
7. Author(s) *Jonathan R. Scheffe*		8. Performing Organization Report No.
9. Performing Organization Name and Address *University of Florida, Division of Sponsored Programs* *207 Grinter Hall* *Gainesville, FL 32611-5500*		10. Work Unit No. (TRAIS) 11. Contract or Grant No. *Master Agreement #: BDV31-977 – 78*
12. Sponsoring Agency Name and Address Florida Department of Transportation 605 Suwannee Street, MS 30 Tallahassee, FL 32399		13. Type of Report and Period Covered *Final Report* *6/2017 - 2/2020* 14. Sponsoring Agency Code
15. Supplementary Notes		

16. Abstract

In this project, photoluminescent stones and solar photovoltaic modules by Wattway were investigated as a means to provide lighting to pedestrian areas and heavily trafficked roadways/pathways. The photovoltaic modules by Wattway were not able to be delivered as scheduled because of manufacturing defects and thus this phase of the project was put on hold. Three large-scale photoluminescent stone installations were installed; two at the Florida Department of Transportation's (FDOT) Traffic Engineering Research Laboratory(TERL) facility and one at the University of Florida. The stones that were used were supplied by Ambient Glow Technologies and were selected from a large number of potential suppliers. Based on our assessment of their luminance and slow decay times, these stones were deemed the most promising to provide light for the longest duration possible; under controlled laboratory conditions, the stones were visibly emitting light for over 12 hours. At TERL, the stones were utilized in concrete and asphalt pathways that were 150-ft. and 200-ft. in length, respectively. Overall, both installations indicated that the stones were stable and no notable degradation in performance was observed. However, because of the ambient lighting at TERL, assessment during the night was difficult and led to the construction of a 30-ft. installation at the University of Florida, where stenciled designs were implemented. Overall, results indicate that the emerald green stones from Ambient Glow Technology provide lighting capable of being observed, albeit faintly, for the duration of the nighttime. Further research should be completed at a larger scale to determine the effect of vehicular travel, driver awareness/human factors and target value for pedestrian or other trafficked pathways. Further, an evaluation of surface integrity with respect to particle attrition and raveling and/or delamination are not well understood.

17. Key Word *Solar, lighting, photoluminescent, sidewalk, asphalt, concrete, roadway*	18. Distribution Statement No Restrictions		
19. Security Classif. (of this report) Unclassified	20. Security Classif. (of this page) Unclassified	21. No. of Pages 101	22. Price

Acknowledgements

This work was supported financially by The Florida Department of Transportation (FDOT) under Task Work Order #: 977 – 78. This project was the result of hard work from a large number of graduate and undergraduate students, without which this project would not have been possible. These students include Rishab Ramaswamy (MS thesis), Elizabeth McMaster, Collin Hamilton, Diego Gordon, Brian Kusnick (bachelor thesis), Amy Bohinsky (bachelor thesis), Zorana Visic, Ali Rahal, and Martin Ngyuen. We also wish to thank Ronald Chin for managing the project and several staff members from FDOT's Traffic Engineering Research Laboratory (TERL) location, especially Mathew Dewitt and Carl Morse, who helped with the installation and maintenance of the concrete and asphalt pathways.

Executive Summary

This project was motivated by the desire to provide lighting to pedestrian crosswalks and other roadway and pathway applications that are not dependent on the electrical grid, in case of a natural disaster. Two solutions were investigated: a solar photovoltaic roadway technology developed by Wattway and photoluminescent stones that are charged during the day and emit light of various colors during the nighttime. Installation of a solar crosswalk with battery storage and integrated lighting and two photoluminescent stone projects, one asphalt and one concrete, were to be constructed at the Florida Department of Transportation's Traffic Engineering Research Laboratory (TERL) facility in Tallahassee. During year one of the project, plans for the crosswalk were jointly developed by the University of Florida and Wattway engineers. However, because of manufacturing difficulties, Wattway cancelled all of their ongoing projects worldwide and that phase of the project was not continued. In parallel during year one, samples from several photoluminescent stone providers were evaluated in the laboratory to determine their spectral properties and luminance versus time. Overall, samples from Ambient Glow Technologies were the best performing in terms of overall luminance and rate of decay; their Emerald Green stones were chosen for construction at FDOT's TERL. A 150-ft. sidewalk and 200-ft. asphalt pathway were constructed, and monitoring equipment was installed to take time-lapse photography and monitor the solar irradiance so that performance could be quantified as a function of weather conditions. A second, 30-ft. concrete installation was installed on the University of Florida's campus in order to better assess the performance with less ambient light and to evaluate the use of templated designs. We chose a UF logo alternating with a high density spread of stones, like that shown below. Results indicate that the stones glow for the duration of the nighttime but become very faint after midnight. Depending on the application, these stones would be suitable to provide warning lighting for drivers, bicyclists and pedestrians for the duration of the nighttime, even on days with little sunlight due to cloud cover. However, the user should evaluate and/or consider other alternate means to illuminate pathway areas of interest to compare economics and benefit recognized.

Table of Contents

List of Figures

List of Tables

Chapter 1 **Introduction**

In a prior project entitled "Integrated Solar Lighting for Pedestrian Crosswalk Visibility" (Project BDV31-977-62), the Florida Department of Transportation (FDOT) was interested in assessing the viability of integrating solar panels into roadway surfaces, specifically at pedestrian crosswalks and other traffic bearing areas. The goal was to provide power for lighting and/or illumination using integrated lighting to enhance pavement markings and visibility, which also could provide service during power failures and in remote areas without nearby electrical utilities. FDOT was primarily interested in technologies that may be integrated directly into the surface of the crosswalk or pavement and not using solar power from external sources (e.g., solar panels next to the road).

The conclusions of this report indicated that there are two viable technologies that provide the best opportunity to meet the FDOT's goals. The first is a slim photovoltaic module produced by Colas that sits directly on top of the roadway surface. See Figure 1-1 below for an example of the technology.

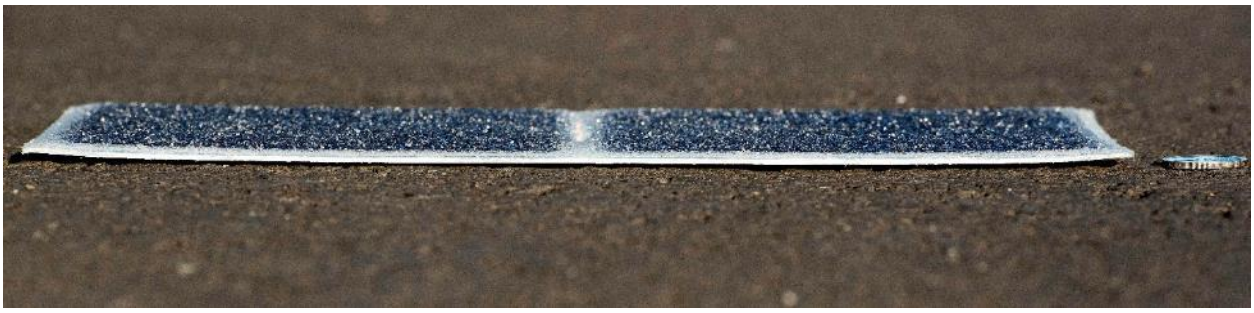

Figure 1-1. Colas's solar module is designed to be placed directly on top of the asphalt[1]. The design is streamlined, as indicated by the thickness relative to the coin on the right side.

The advantage of this, compared to other competing technologies, is that installation is possible without a complete overhaul of the entire roadway surface; products offered by competing companies such as Solar Roadways® and SolaRoad are designed to replace the entire roadway surface, and installation is expected to be costly. Colas's solar module has recently been integrated in large scale roadway projects in Georgia[7] and France[4] for power production. The French installation was a 1-km stretch of roadway in Normandy that cost roughly 5 million USD (see Figure 1-2 to the left). The most ambitious project utilizing this technology is currently supported by the French Minister of Ecology and Energy and promises to develop a 621-mile stretch of solar roadway in France.

Figure 1-2. Image of a 1-km stretch of solar roadway surface in Normandy, France, completed using Colas's solar modules[4].

The second viable technology is a passive approach that takes advantage of photoluminescent stones. This technology is not capable of producing power, but rather the photoluminescent stones absorb sunlight

Figure 1-3. Nighttime photograph of the photoluminescent "Van Gogh – Roosegaarde Cycle Path".[3]

during the day and glow during the nighttime[8]. No active energy storage is possible and therefore the duration of lighting may be limited. Furthermore, control of light emittance is not possible like it is with LED's driven by a solar roadway panel. The main advantage of this technology compared to photovoltaic technologies is related to the lower cost of materials and it has been utilized successfully for bike paths in the Netherlands. For example, a collaboration between Hejimans and Studio Roosegaarde conceived of and constructed the "Van Gogh – Roosegaarde Cycle Path", as shown to the left in Figure 1-3[3]. Furthermore, it has recently been demonstrated by the Texas A&M transportation institute on their campus (https://www.fastcoexist.com/3067911/heres-the-first-glow-in-the-dark-bike-lane-in-the-us).

The aim of this project is to construct two pilot facilities based on these candidate technologies at the FDOT's Traffic Engineering Research Lab (TERL) in Tallahassee, FL. The first involves integrating Colas's solar panels into an already established pedestrian crosswalk and coupling this technology with battery storage, LED lighting for alerting oncoming traffic and powering overhead lighting. The system size will be designed based on solar radiation predictions from monthly averaged models and performance will be measured in terms of energy production and durability. The second involves constructing a small portion of sidewalk with commercially available photoluminescent stones to measure their performance in terms of durability and emittance duration during nighttime.

Chapter 2 **Solar Crosswalk by Wattway**

Preliminary Solar Crosswalk Design

During a productive meeting at the TERL laboratory on September 20th 2017 that included representatives from Wattway, FDOT and the University of Florida, the location and underlying design of the solar powered crosswalk were discussed. Here it was decided that the optimal location of the crosswalk would be located at Test Bed #1 indicated below in Figure 1 that is located to the West side of the main building at the TERL site. The site was primarily chosen because of the overhead lighting in place that will be powered by the Wattway solar panels.

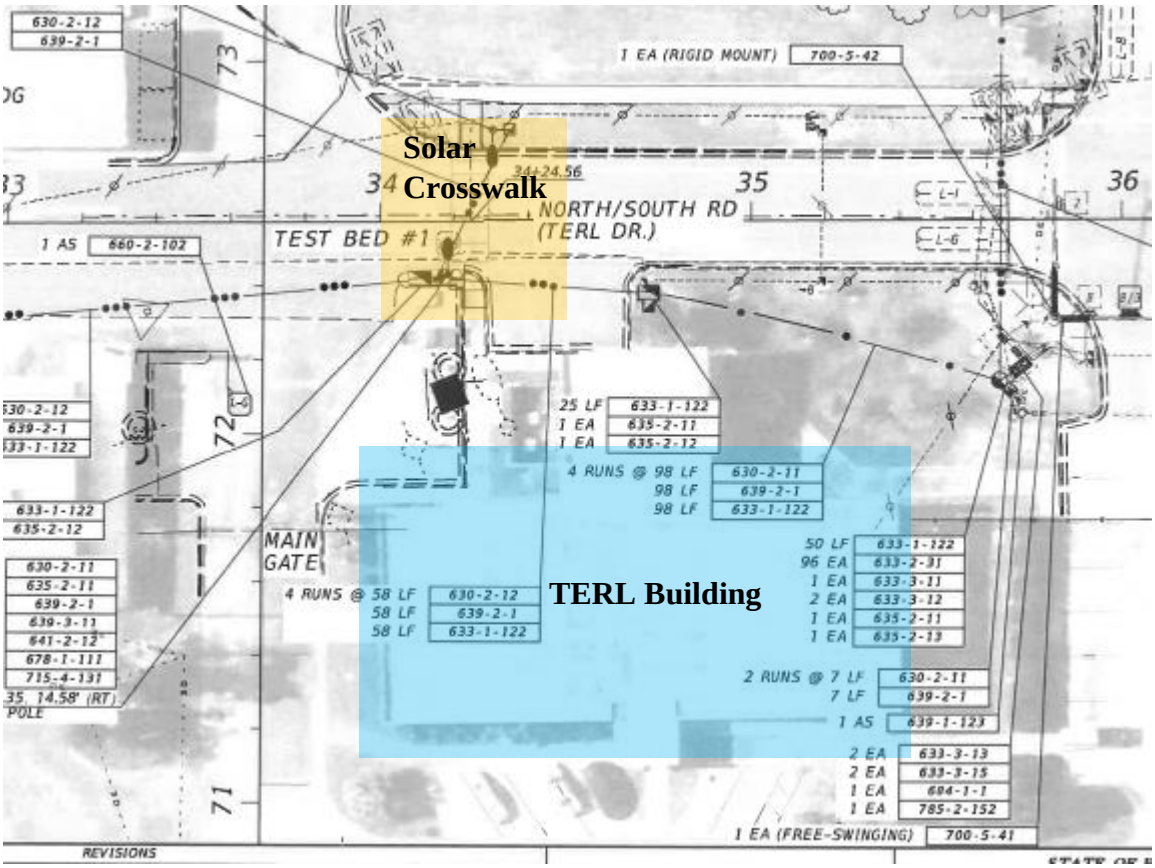

Figure 2-1. Blueprint of the TERL facility. The solar-powered crosswalk will be placed at Test Bed #1 on the west side of the main TERL building where overhead lighting is readily available.

In total it was decided that there will be 30 m^2 of Wattway panels installed at the intersection and to maximize the length of roadway that the panels are placed on (in order to maximize the length during which traffic slows or accelerates), all of the panels will be installed on only one side of the road (West Side). This will also reduce the number of in-road LED lights required and other peripheral equipment. It was discussed that this will be especially important for the friction testing that will be conducted by the FDOT Materials office using a locked-wheel measurement technique. In order to have a single contiguous surface and because of the fixed dimensions of the solar panels, the panels will be placed on the sides of the road entering and exiting the crosswalk. This is necessary because within the crosswalk itself are painted pedestrian crossings with fixed width spacing between them of different dimensions than the panels. Half of the panels will be placed on the side of incoming/decelerating traffic and half on the side of

outgoing/accelerating traffic. This distinction will prove to be valuable when processing the friction testing results during the year following construction. Two rotatable, stainless steel LED road studs (TS-SR-50, Traffic Safety Corporation) will be installed in the roadway surface on the side facing incoming traffic that will blink during pedestrian crossing. Pedestrian crossing will be automatically detected by photo sensors (Pedestrian Detection Photo-Sensor Bollards, Traffic Safety Corporation) placed at the entrance of the crosswalk on the side of the road where it is installed. LED lighting and sensors, as well as the already installed overhead lighting will be powered during off-sun hours with a battery bank of sufficient load.

A drawing of the crosswalk layout is shown in Figure 2-2. As seen the panels (each 0.7 m by 1.4 m and 1.0 m^2) are arranged in a manner where half are placed on the side of incoming traffic and half exiting traffic, with lighting placed between the crosswalk and the panels on the incoming traffic side. In addition to the in-road LED lighting, photo detectors and the battery bank, several devices specific to the Wattway installation will be placed within a power cabinet. These include:

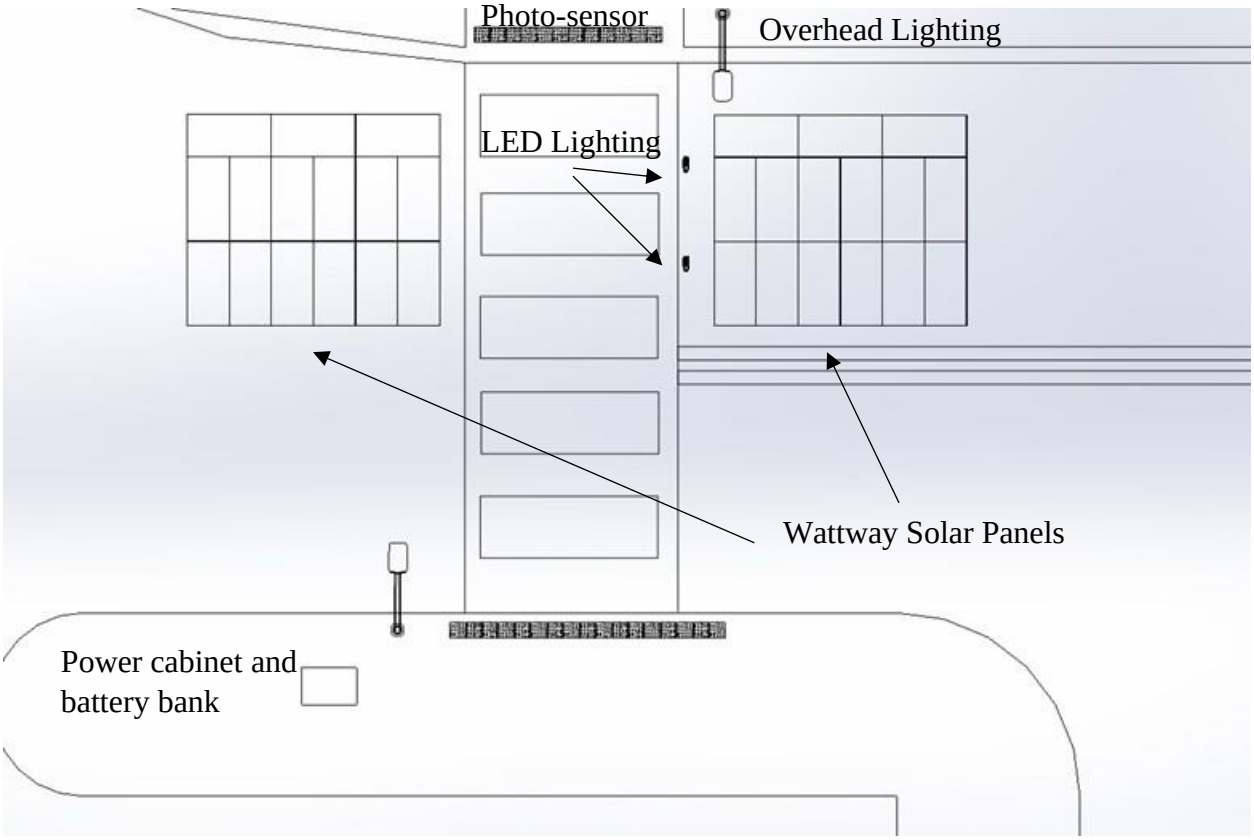

Figure 2-2. Layout of solar-powered crosswalk with solar panels located on each side of the pedestrian crossing, in-road LED lighting, overhead lighting. and motion sensors, all powered by a battery bank**.**

- Vaisala Weather Transmitter WXT520: is a lightweight transmitter that offers six weather parameters in one compact package. It measures wind speed and direction, precipitation, atmospheric pressure, temperature and relative humidity.
- Heat sensors to verify the internal temperature of the monitoring cabinet PT 100 4/20 mA
- A Digital Silicon Irradiance Sensor of Ingenieurbüro (Si-RS485-TC-T)

- Phoenix Contact Measuring instrument (ref: EEM-MA600-2901366), with its current transformer (ref: PACT RCP). The transformer measures the Wattway production of electricity
- Webdyn device (provided by Wattway)
- A transformer (AC to 24V DC) to adapt the input power for the monitoring devices
- 1 Fan for a Temperature regulation in the Electrical cabinet
- A switch for switching on/off the entire monitoring cabinet
- Circuit breakers
- Lightning arrester
- Fuse holders

A local Tallahassee contractor (Ingram Signalization) was designated to perform all of the electrical work and hardware installation (minus the solar panels) and is to work closely with Wattway to determine all of the specific components not specified here: these include the battery bank and power cabinet. After discussions with Wattway and Ingram, as well as others present during the on-site TERL meeting on 9/20/2017 it was concluded the most reasonable option for this project is to size the battery bank large enough to power the devices necessary but not all of the power received by the Wattway panels – this would become unnecessarily expensive. The excess power will be directly delivered to the main TERL building on site.

While we hoped to have all of these final specifications established by 11/1/2017, the discussion between Wattway, UF and Ingram proved to be slower than anticipated and much of the installation that was originally thought to be completed by Wattway has been shifted to UF and/or Ingram. For example, the electrical power cabinet, components and design needed for monitoring and controlling the distribution of power from the Wattway installation were not to be provided by Wattway as expected. We expect however, that all of this is finalized before the end of 2017. Wattway has completed the designs for the electrical work and once the specific power cabinet and battery bank are determined, all components will be ordered and soon followed by installation early 2018. The preliminary electrical designs provided by Wattway are shown below in Figure 2-3.

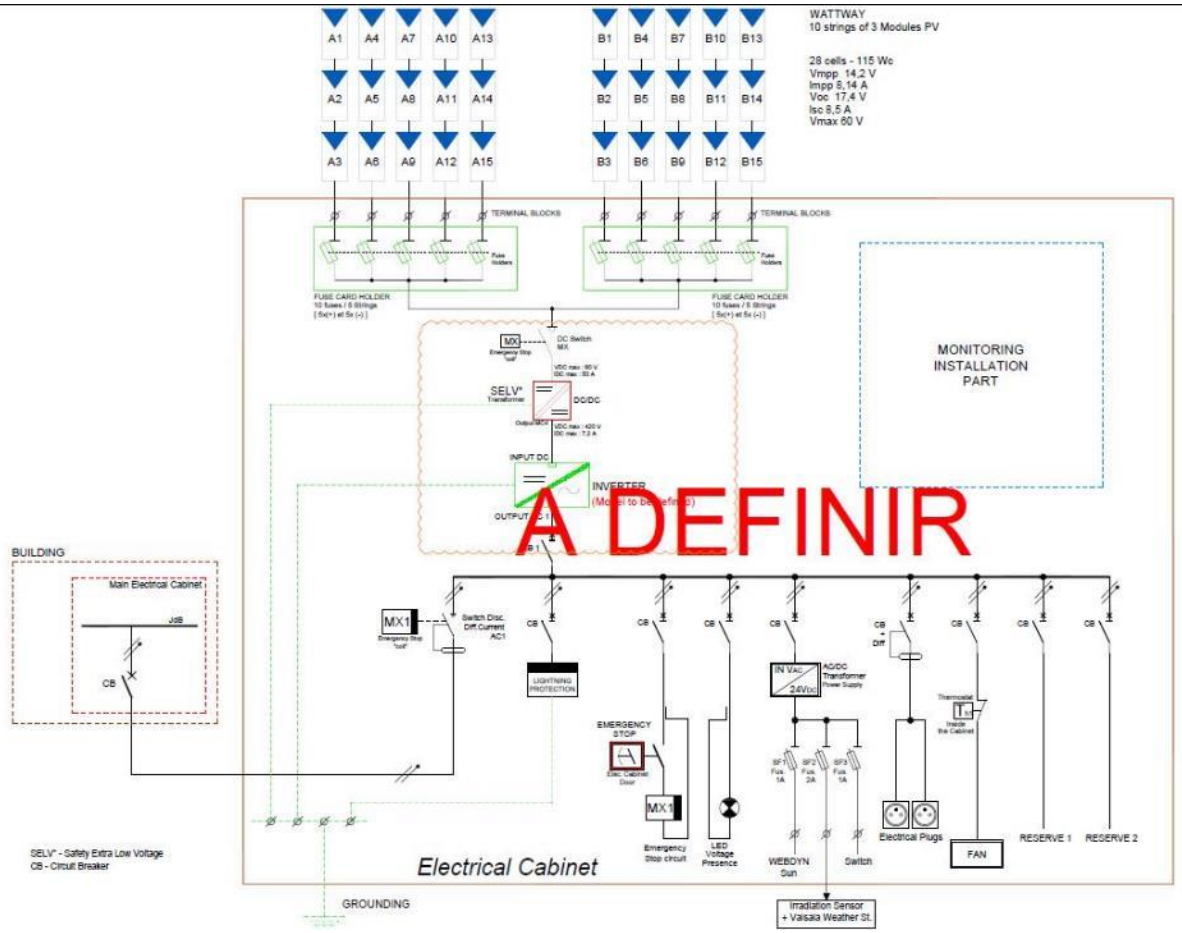

Figure 2-3. Overview of the electrical layout of the Wattway solar panels. Excess power will be relayed to the TERL main building.

Issues with Wattway Installation and Cancellation of Contract

After several back and forth discussions with Wattway representatives between 11/01/2017 and 8/10/2018 it became increasingly difficult to maintain contact with Wattway and communication between them and Ingram signalization was minimal. There were several delays for one reason or another regarding designs or specifications and then on 8/10/2018 I received notification from my primary contact at Wattway that he would be leaving the company and would no longer be involved in the design. At this point I was put in touch with a new project manager who wanted to begin the design from scratch, undoing months of negotiations and back and forth between

Wattway, Ingram and the University of Florida. Ultimately, on 8/20/2018 I was told that there were further delays with the contracting (which was delayed month by month from the beginning) because of difficulties working in the United States as a French company with US subsidiary. At the same time I was notified that Colas needed to perform further tests of the asphalt for "deflection (stiffness) and geometry (flatness/roughness" to ensure it was suitable for their technology. This was never initiated at the beginning of the project one year prior and no reasoning was provided. Nevertheless, after the nearly year delay and then new issues arising with contracting and ensuring asphalt quality I was beginning to doubt their ability to follow through with the promise of installation. Following this there were new issues arising weekly related to new electrical requirements, or component requirements that Ingram would ultimately be responsible for installing, overall creating a cloud of confusion on their end. Ingram provided us with new quotations, FDOT was able to deliver on the asphalt testing, but in the end there were always more questions and new specifications that Wattaway was proposing. For example, on 9/26/2018, Wattway informed us that heavy trucks could not drive on the installation, but this was never indicated prior and not compatible with operations at TERL. Finally, on 11/12/2018 the reason for the back and forth became more clear, as Wattway was cancelling all of their installations. The email was as follows:

"*I regret to inform you that our Technical Committee has lately decided to put all our current projects on hold until next spring.*

On several projects we have seen some minor defects that need to be fixed before we go any further.

From a technical point of view those defects consist of small debondings on the edge of the Wattway modules. This doesn't affect the safety and production of energy but it is very likely that such defect will lead to premature failure. More specifically the thermo-mechanical behavior of the module is pointed as the main cause and some solutions are already being implemented and tested.

The fact is that the testing and qualification process will takes several weeks (fatigues/aging...) and in the meantime we won't be able to carry out any project.

Following the recommendation of our scientists and researchers and in compliance with our quality policy we have decided to temporarily freeze the production of the Wattway panels.

This period of time is necessary to proceed as follows:

- *Stop all new installation of pilot site*
- *Analyze malfunctions*
- *Adapt and modify materials*
- *Revise some steps of the installation method*
- *Validate new solutions*
- *Re-start the production*
- *Continue new projects.*

This temporary interruption:

- *Will not modify the price*

- *Will allow each of ours early adopters to benefit from our latest technology and return on experience.*

Though this temporary setback isn't welcome and will compromise some projects we believe that this is a necessary measure.

I am fully aware that this decision is falling at a very bad time after all the recent joint efforts in successfully assessing the job site.

I remain at your disposal to provide you with more information and discuss this in greater detail."

After this delay and all of the prior delays, we discussed with Ron Chin and other project managers from FDOT that it would be in the best interest of the project to cancel all deliverables related to the Wattway installation and focus solely on the photoluminescent installations.

Chapter 3 **Photoluminescent Stones as Construction Materials for Sidewalks and Roadways**

This work explores the future possibility of integrating long afterglow photoluminescent materials (phosphorescent) onto sidewalks and asphalt roadways or bikepaths as a nighttime visibility aid. Various photoluminescent sample (stones and powders) having different glow colors, sizes, geometries and procured from a variety of distributors have been tested for their luminance and spectral properties in the laboratory. The most promising materials have then integrated into concrete and asphalt in different configurations in order to assess their aforementioned properties. These results will be used to predict the most viable configuration to be used in a large scale test facility at FDOT's TERL facility in Tallahassee.

Nighttime visibility poses a problem on many streets where street lighting is not present or is simply not sufficient and phosphorescent materials may provide a cost effective solution in many cases. However, there are uncertainties regarding commercially available phosphors that present themselves; the most typical are their light levels, the rate of decay, and the ease of placement in concrete/asphalt. To address these issues, a new experimental setup has been developed to gather and analyze luminance, spectral and asphalt/concrete stability data.

We aim to identify candidate suppliers of photoluminestcent stones that may be suitable for installation in concrete and asphalt construction projects. Upon identification of candidate materials we aim to test their spectral properties, identify those with the highest luminance and longest luminance decay and integrate the most promising materials into laboratory scale concrete and asphalt "coupons" to evaluate different synthesis methods. Ultimately, we aim to determine the most suitable stones to be utilized in a scaled up construction project at the Florida Department of Transportation's TERL facility and evaluate their performance by coupling time lapse photography measurements with measurements of global horizontal solar irradiance.

Photoluminescent Materials: Background

Photoluminescent materials, also called phosphors, are divided into fluorescent and phosphorescent categories. Fluorescent materials emit light while they are being excited by a light source and have a very small afterglow lifetime (light emitted after the end of excitation). An example of such a material is Y_2O_3:Eu^{3+} which is used in fluorescent lamps with more examples present in a paper by Feldmann et al.[9]. Phosphorescent materials do not emit light while they are being excited. Instead, they store the excitation energy and emit light only after the excitation source is removed. An example of such as material is europium and dysprosium doped strontium aluminate phosphor ($SrAl_2O_4$: Eu^{2+}, Dy^{3+}) which has the ability to emit light throughout the night[6, 10].

Phosphorescent materials have also been in use as lighting aids for a long time with ZnS: Cu being an early glow in the dark material used in watch dials[11]. This phosphor however, did not have the ability to glow for a long time period after being excited with an afterglow period lasting about an hour. Addition of radioisotopes enhanced the glow[11] but that does prove an environmental friendly option. This led to the search for longer glowing materials such as Strontium Aluminate phosphors which are environmental friendly and have high stability[11]. These also have the ability to emit a perceptible glow up to 12 hours after excitation[6] which make them a good option for visibility applications. A more important usage of such phosphors however, has been in exit guideway systems for evacuation purposes[12]. For a detailed account, the reader is encouraged to refer a paper by Jeon and Hong[13] which speaks about their use in impaired visibility situations. Other applications include their presence in barricade warning

lights as suggested by Wong[14] and along the side of highways to provide visibility to vehicles[15]. These have also been placed onto bike lanes as on Texas A&M's campus[16]. In addition, they are also supplied commercially as was discussed above which makes them useful for residential applications as well.

Mechanism of Phosphorescence

A phosphorescent material is composed of an insulating crystal (such as $SrAl_2O_4$) which is doped with suitable impurities or dopants (Eu and Dy) to give it luminescent characteristics. The phosphor $SrAl_2O_4:Eu^{2+}$, Dy^{3+} has been researched by a number of researchers[6, 10, 11]. The ability of the dysprosium ions to act as traps leads to its long afterglow which is the reason for its suitability for applications as discussed in the previous section. Various other phosphors have been researched with a paper by Clabau et al.[11] listing a variety of such materials. The strontium aluminate phosphors are the most widely available and most viable of the entire list and hence, the focus would be on their phosphorescence mechanism which is discussed below.

A mechanism has been shown in Figure 3-1 which has been adapted from Yuanhua Lin et al.[5]. In the case of $SrAl_2O_4:Eu^{2+}$, Dy^{3+}, the europium ions act as activators which cause luminescence in otherwise non- luminescent strontium aluminate; the host material. The dysprosium ions act as hole capturing agents, which leads to the phosphorescence. They reside in traps which Randall and Wilkins[17] describe as discrete energy levels within the material, due to crystal defects produced by the dopant. Upon excitation, the Eu^{2+} ions undergo an electronic transition from the 4f level to the 5d electronic level. These ions in their excited state, capture electrons from the valence band of the host material. This causes vacancies in the valence bands, called holes. Matsuzawa et al.[6], suggest that these holes get thermally released into the valence band and are then captured by the Dy^{3+} ions. When the excitation light source is removed, these holes get released back to the valence band and migrate through it to combine with the excited Eu^{2+}. This causes charge carrier recombination and thereby leads to the phenomenon of luminescence. We can say that the trapping of the ions by Dy^{3+} prevents light emission during excitation while the afterglow occurs due to the slow release of holes and the recombination. The depth of traps and the number of traps can greatly influence the release of charge carries from them. Further there have also been studies on the effect of temperature on the release of charge carries from them. Both of these questions are answered in Randall's work[17].

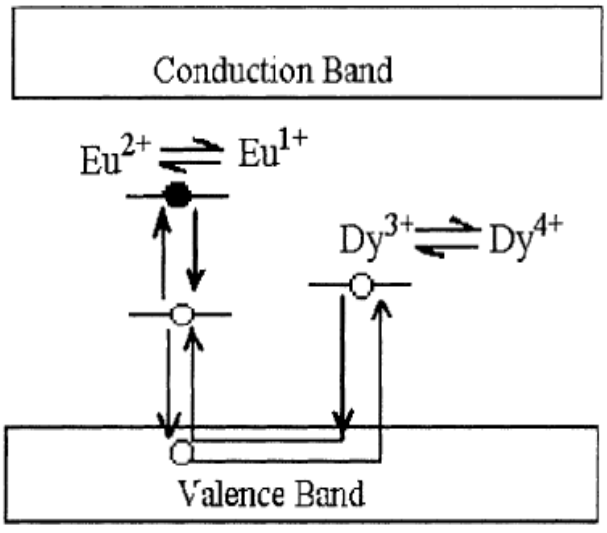

Figure 3-1. Afterglow mechanism for $SrAl_2O_4$: Eu^{2+}, Dy^{3+}, from Lin et al.[5]

Another interesting aspect pertaining to photoluminescent materials is the Stokes Shift[18]. This is the difference between the maxima of the excitation and emission bands. This is usually measured in cm^{-1} and its value is usually bigger if there is a significant difference between the bonding in the excited and ground

states. This also requires an understanding of the electronic transition mechanisms resulting in emission, and for those, the reader is encouraged to refer to Blasse and Grabmier's work[18] and Cees Ronda's theory on luminescence[19].

Luminance Background and the Sensitivity of the Eye

In the lighting world, two types of quantities are important, with those being radiometric and photometric[20]. Radiometric quantities cover the entire electromagnetic spectrum of light, while photometry is only concerned with what the human eye can perceive. The photometric aspect is pertinent as far as afterglow materials are concerned because we are only concerned with the visible portion of light emitted by the material. Hence, photometry aspects would be considered here, and a detailed account of them can be found in Schubert[20]. The lumen is the visible element of optical power (W). Built on it is a quantity called luminance (L) and this would be the most relevant photometric term for this project. This is the luminous intensity per unit projected area leaving a surface. Simply put, it is the lumens of light per solid angle leaving the surface projected in a specific direction. It is measured in cd/m^2. Schubert, in his book on light-emitting diodes[20], also lists the radiometric equivalent of luminance, which is the radiance. Other equivalent parameters for other photometric terms can also be found there, which may enable the reader to get a clearer picture.

The luminance varies on the basis of the color of light leaving a surface because the eye is more sensitive to certain colors than others[21]. In fact, if equal amounts of energy from blue and green were to be incident on the eye, the response of the eye would not be the same for both of those colors. This occurs due to the presence of rods and cones in the retina. To study this in more detail, the International Commission on Illumination (CIE) developed photopic and scotopic curves which describe the sensitivity of the eye to different wavelengths. The photopic curve applies for $L > 3.0$ cd/m^2 where cones are used, while the scotopic curve is used when $L < 0.001$ cd/m^2. In this case, only rods are used. For the middle range, a mesopic curve exists which has been described by Barbur and Stockman[22].

The photopic and scotopic curves are utilized more widely, and hence, we will focus on them. Consider Figure 3-2, which shows the photopic curve that was adapted from Modest's book on radiative heat transfer[2]. The x-axis shows the visible wavelength range while the y-axis shows the values for the luminous efficiency, or the eye sensitivity function, $v(\lambda) = K_\lambda/K_{max}$. This is a parameter that ranges from 0 to 1. The CIE states that at 555 nm, $v(\lambda)$ would have a value for 1, if the photopic curve is considered. This would mean that the color green would produce the highest impression of brightness. The same value would apply for 507 nm when the scotopic curve is used[19]. This leads us to a parameter called the luminous efficacy (K_λ)[20]. This is the ratio of the luminous flux (lumens) to the radiant flux (W) with the expression depicted by Equation 1-1.

$$K_\lambda = \frac{683 \int v(\lambda)P(\lambda)\, d\lambda}{\int P(\lambda) d\lambda} \qquad (1\text{-}1)$$

The CIE specifies that there are 683 lumens/W at 555 nm, if the photopic curve is used. The efficacy for all other wavelengths is then scaled on the basis of respective $v(\lambda)$ values, with the rest of the equation parameters remaining the same. $P(\lambda)$ is the spectral radiant power over the entire range of light radiation emitted by a material, and an expression can be found in Murphy's work[23]. The luminous efficacy is relevant for this study because it tells us about the amount of

lumens present per watt of power. The lumens dictate the brightness of light falling on the eyes and hence they give us a picture about why certain colors have different reception abilities.

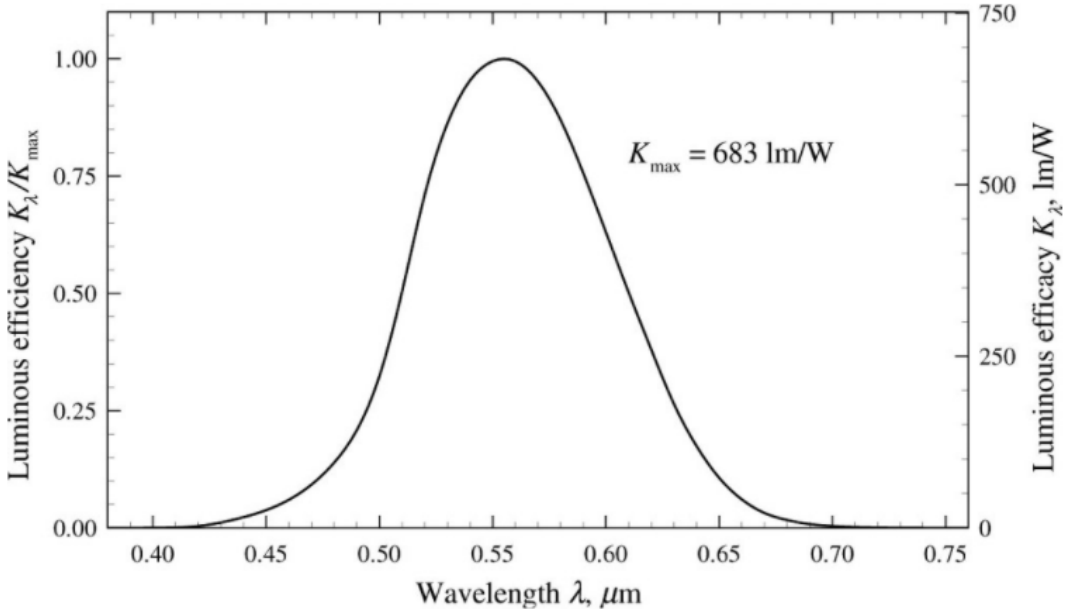

Figure 3-2. Efficiency functions (y axis) for photopic vision, adapted from Modest[2]. The efficacy is listed on the right-hand side with the highest value being at 555 nm.

Luminance and Spectral Measurements of Candidate Samples

Experimental Methods

Experimental Setup

Figure 3-3 shows the experimental setup that was developed to measure spectral properties (i.e. color) and luminance versus time. The experiments were carried out in a black optical enclosure procured from Thor Labs Inc. This was important as a black enclosure prevents the samples from getting continuously charged from the ambient light. It also ensured that the samples were

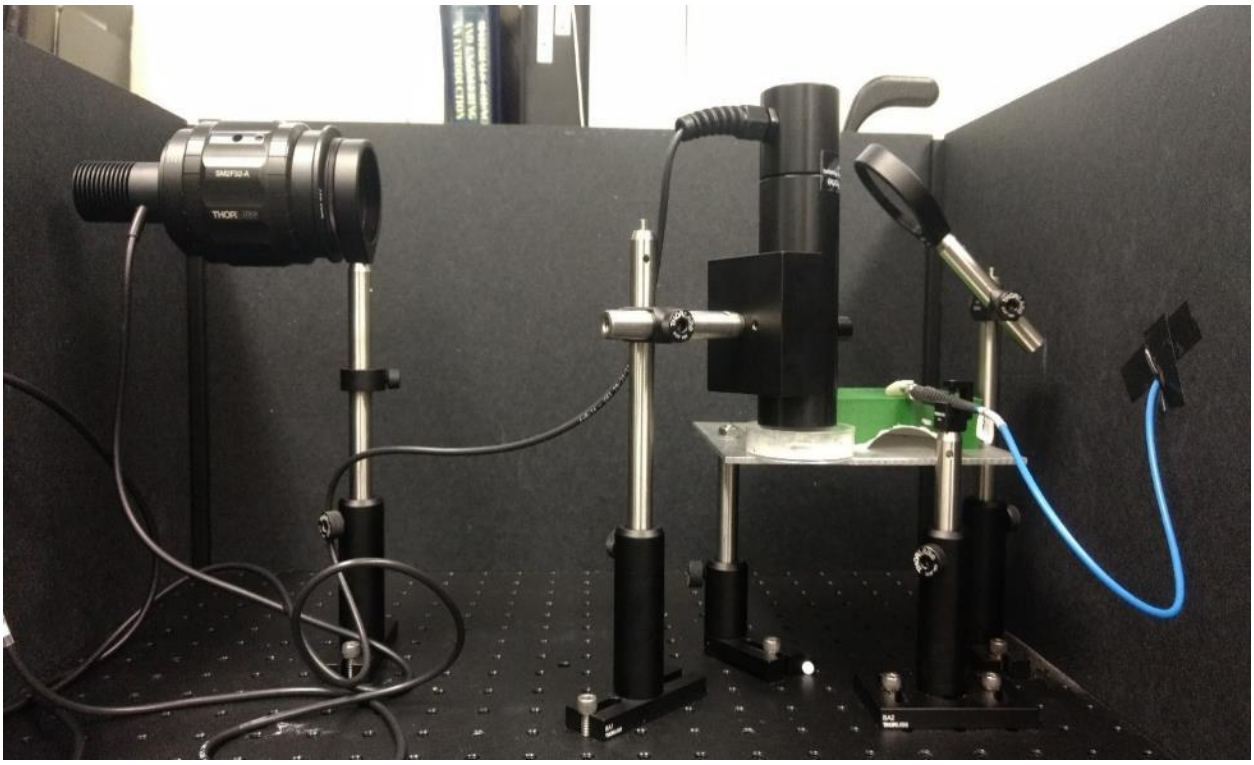

Figure 3-3. The experimental setup. The light from the LED arrives at the mirror which reflects it downwards. An optical fiber can be seen touching the stone to make spectral measurements.

discharged prior to all tests[11].

To illuminate the samples, a Neutral White LED was used which had a wavelength range of 400-700 nm. The LED was coupled with a collimator which worked to collimate the beam, and an LED driver which controlled the power output. The maximum power output of the LED after collimation was measured with a S314C Thor Labs thermal power sensor and was found to be 264.5 mW with an output flux of 233 W/m^2. The light from the LED was then directed onto the sample placed on a mounting table after reflection from silver coated plane mirror set at 45 degrees. The mirror has a 2 inch diameter and was again procured from Thor Labs Inc.

A Mightex CCD Spectrometer was used along with an optical fiber to capture the emission spectrums (color) from the samples. The spectrometer comes with a built in software system which allowed for the identification of emission peaks on a computer. The slit width used for light entry was 25 µm which enables good resolution while the fiber optic had a diameter of 400 µm. For the luminance studies, Delta Ohm Technologies' HD2302 radiometer was used. The

meter was coupled to a luminance probe having a measuring angle of 2 degrees and an entrance aperture of diameter 18 mm. A luminance meter aligner was used to direct the light efficiently into the probe, to address the small measuring angle. This has been discussed in the later sections.

Samples and Distributors

Figure 3-4. Size specification for samples. From left to right: powder, 1-mm pebble, 3- to 4-mm stone, 5- to 8-mm chip, 5- to 8-mm stone, 11- to 14-mm stone and a 25-mm rock.

Samples having 5 different glow colors were acquired from 6 distributors for the experimental campaign. These were Coreglow, Phosphor Ltd., Ambient Glow, Glowstones, Rare Earth Sciences and Ruby Lake Glass. All samples procured from these companies had various sizes and a sizing specification is shown in Figure 3-4. Table 1 gives the list of distributors and the samples they provided. The samples were designated IDs for keeping track of them on the basis of a nomenclature. The bolds indicate the color of the sample used and the letter following the bold shows the geometry. Additionally, a size range has been shown with the company names abbreviated at the start. As an illustration, CGAC815 would refer to CoreGlow Aqua chips having a size range of 8-15 mm. The reader should note that 'chips' are essentially flat stones. It is important to note that the base host elements for the colors green, blue, aqua and purple are Sr, Al and O. The emission color however is affected by the element concentrations[24].

Table 1. List of samples tested and their distributors

Company	**Sample Color**	**Sample Geometry**	**Sample ID**
Ambient Glow	Aqua	Small stones	AGTAS34
		Medium stones	AGTAS58
		Large stones	AGTAS1114
		Pebbles	AGTAPB
		Powder	AGTAPO
	Blue	Small Stones	AGTBS34
		Medium Stones	AGTBS58
		Large stones	AGTBS1114
		Pebbles	AGTBPB
		Powder	AGTBPO
	Green	Small stones	AGTGS34

		Medium stones	AGTGS58
		Large stones	AGTGS1114
		Pebbles	AGTGPB
		Powder	AGTGPO
	Purple	Small stones	AGTPS34
		Medium stones	AGTPS58
		Large stones	AGTPS1114
		Pebbles	AGTPPB
		Powder	AGTPSPO
CoreGlow	Aqua	Chips	CGAC815
	Blue	Chips	CGBC38
	Green	Chips	CGGC815
		Powder	CGGPO
Glowstones	Aqua	Stones	GSAS815
		Chips	GSAC58
	Blue	Stones	GSBS815
		Chips	GSBC58
	Green	Stones	GSGS815
		Chips	GSGC58
Phosphor Ltd.	Green	Powder	PLGPO
	Red	Powder	PLRPO
Rare Earth Sciences	Green	Rock	REGR
Ruby Lake Glass	Green	Pebbles	RLGPB

Spectral Measurement Procedure

1. All samples were discharged for at least 24 hours prior to testing them. This ensured that the luminance readings acquired were indeed as a result of the material being in its ground state.
2. The average frame number was set to 20 in the software which means that 20 spectrums were averaged to obtain one emission spectrum. The exposure time was set to 6500 ms which was the maximum limit and which works for low light applications like phosphorescence.

3. This was then followed by acquiring a dark spectrum from the samples. A dark spectrum was acquired as the optical fiber recorded a non- zero signal intensity when kept inside the dark enclosure.

4. The LED illuminated the samples for a period of 20 minutes[25] which works as the saturation limit for absorption. It was then turned off for spectrum acquisition.

5. The spectrometer fiber optic was kept normal to the samples with the tip almost touching them to get a strong signal. This was followed by a raw data capture.

6. All spectrums were averaged over 2-3 tests to minimize any variations due to fiber contact with the surface.

The raw data also has vertical lines in the spectrum due to the dark noise. To get the true spectrum, the dark data was subtracted from the raw data to obtain a cleaner curve. Figure 3-5 shows the process.

Luminance Measurement Procedure

1. As in the case of spectral measurements, all samples were firstly discharged for 24 hours.

2. Samples were placed in various petri dishes and their positioning was fixed through a luminance meter aligner which wrapped around the probe. This compensates for the probe's narrow measuring angle of 2 degrees. The number of stones placed in the aligner can vary.

3. The LED excited the samples for a period of 20 minutes and they were then moved under the luminance meter for acquiring readings.

4. Readings were acquired 30 s after excitation had ended to allow time for the movement of the sample from under the LED to the meter probe. These were acquired for a period of 10 minutes.

5. Readings were subtracted from a dark luminance value of 0.3 cd/m2. This is the value displayed by the device when there is not lighting present around the probe.

6. All values were converted to the mcd/m2 scale. The log of luminance values was then plotted against the log of time (minutes) to interpret the decay curves. A second order polynomial curve was used to fit the points[26].

7. The polynomial curves for some samples were also extrapolated till a value of 3 mcd/m2 was reached. Visually, this value represents a full moon on a street with no other lighting source present[20]. Hence, this value is of significance. In this chapter, only one sample's luminance was

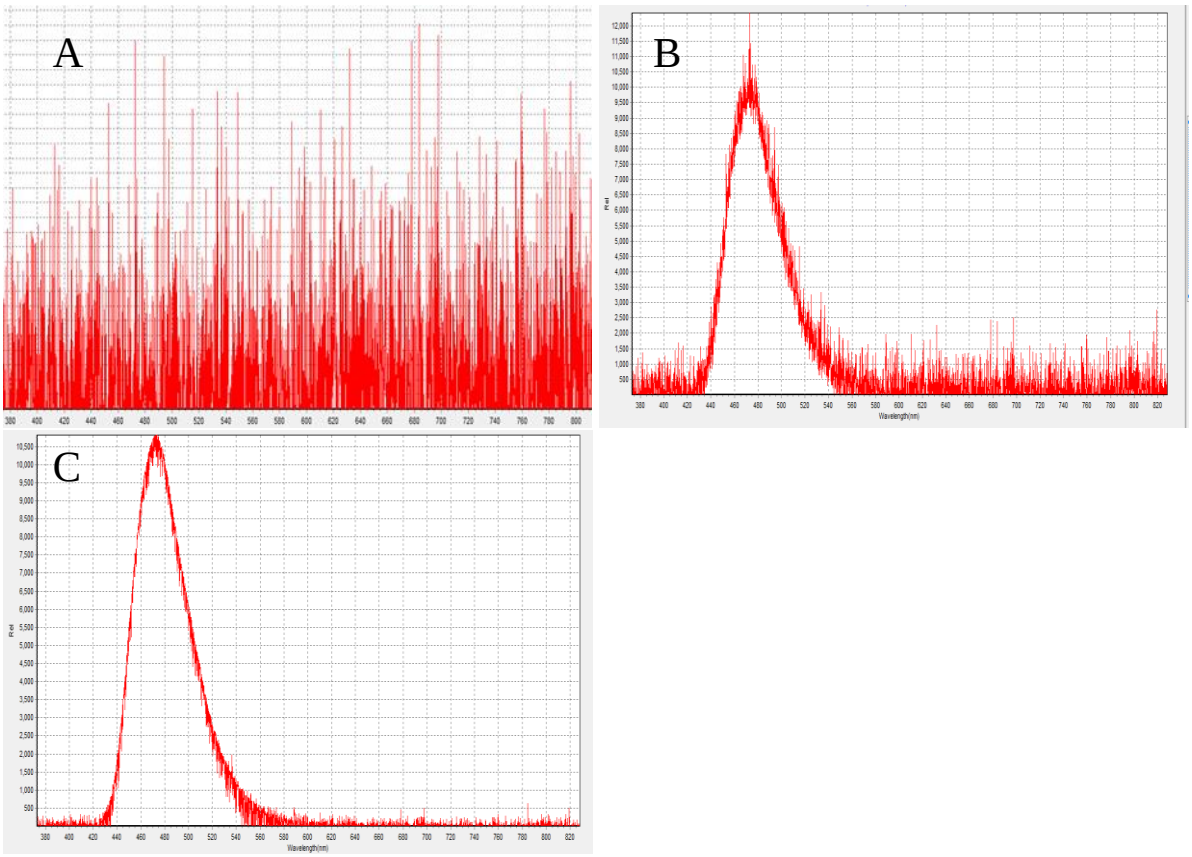

Figure 3-5. Spectrum Capture Process: (A) dark spectrum, (B) raw spectrum data, (C) true spectrum

Results and Discussion

Spectral Measurements

From Figure 3-6 (A), we notice that the general emission peak for green is at 515-520 nm with Rare Earth Sciences' sample's peak being slightly shifted at 510 nm. For the color green, Ambient Glow's sample proved the most promising of all the companies as evidenced by the highest peak. We can also observe the spectral distributions for aqua and blue in the Figure 3-6 (B) and (C) with emission peaks for the colors being 496 nm and 473 nm respectively. Here we again notice the same behavior for Ambient Glow's samples when compared to other companies. Finally, spectrums were too noisy for purple and red due to lower light levels and they have been grouped together in Figure 3-7. For all the colors, except red we notice a broad emission band which can be attributed to a large number of trap energy levels within the material. The Dy^{3+} traps can be situated closer or farther away from the valence band which changes the amount of energy needed to release the holes from them[17].

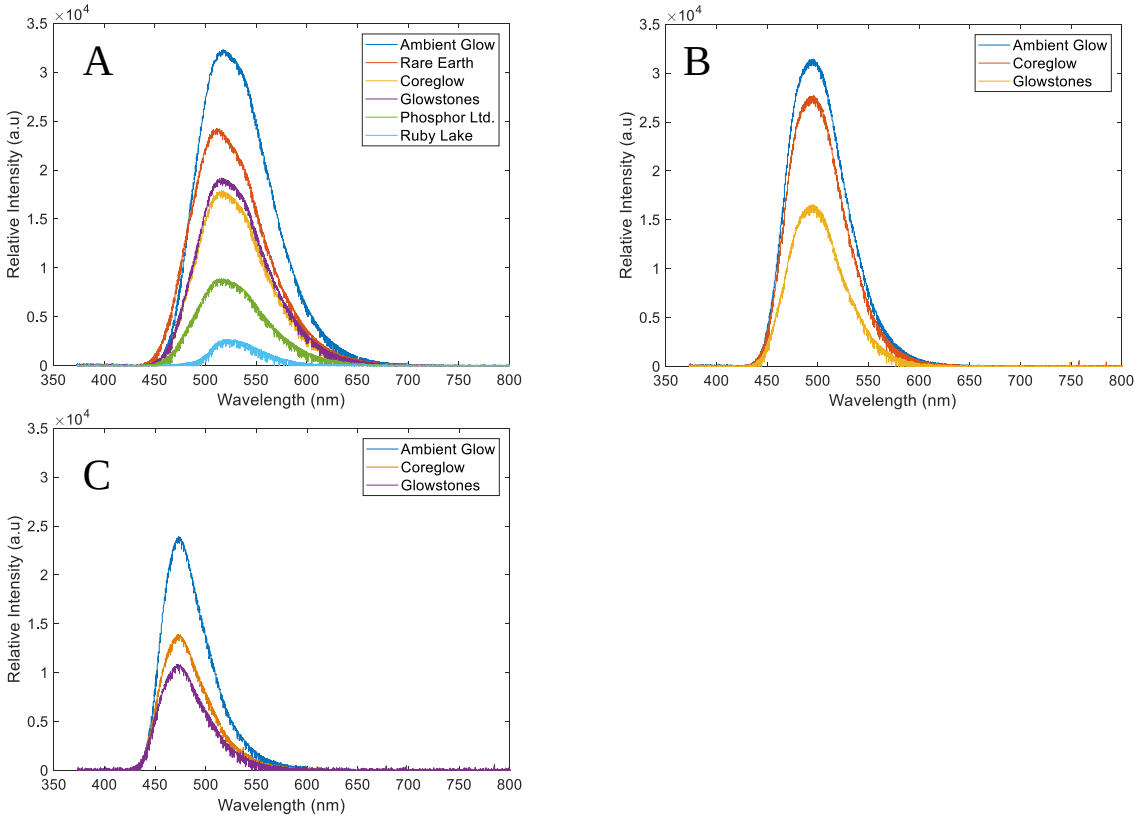

Figure 3-6. Spectrums compared between colors green, aqua, and blue procured from different companies: (A) the spectral curves compared for green; (B) aqua spectrums with the peak at 496 nm; (C) blue spectrums with the peak at 473 nm. Overall, Ambient Glow's samples had the highest intensities and Ruby Lake's were the lowest.

From what was discussed above, we can say that AGT's samples prove the most promising on account of the highest emission peaks. Further, the peak wavelength of its green glowing sample (520 nm) lies closest to 555 nm (maximum spectral sensitivity value) and is hence suitable for the human eye's sensitivity requirements. In addition, the excitation spectrum of the white LED

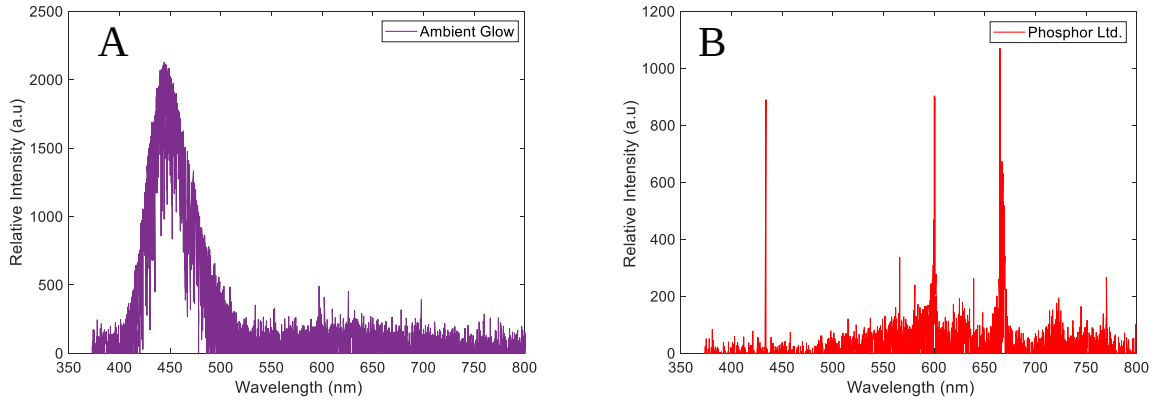

Figure 3-7. (A) Purple spectrum with a peak at 440 nm, (B) Noisy red spectrum

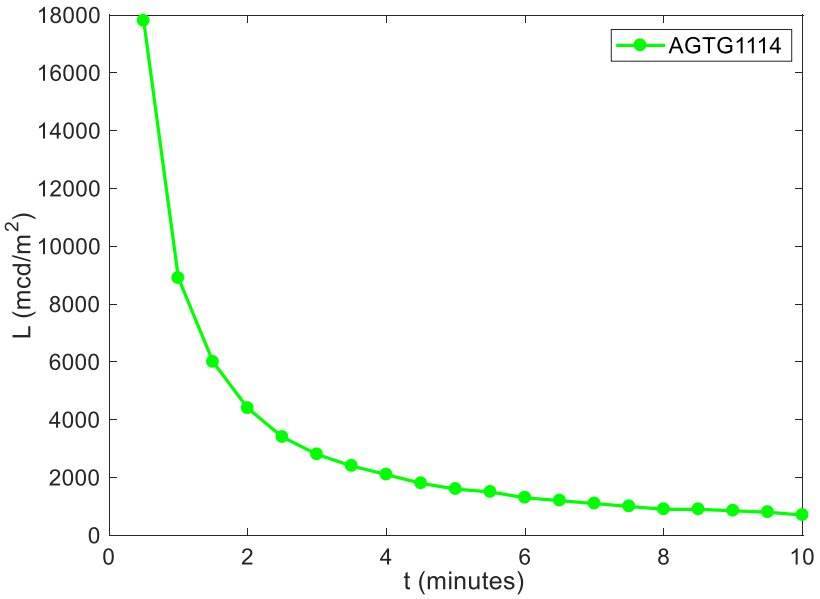

Figure 3-8. Luminance decay trend for Ambient Glow's 11- to 14-mm stones. The trend is dependent on the material, and we observed the same trend for all samples except for the color red.

light source is in the wavelength range is 400-700 nm. Therefore, this full spectrum light source could be used to excite all the colors tested.

Luminance Measurements

A general decay trend for the Ambient Glow's 11 - 14 mm samples is shown in Figure 3-8. The material used over here was the long afterglow $SrAl_2O_4:Eu^{2+}$, Dy^{3+}. Looking at the figure, we can see that the decay is exponential in nature with a rapid rate for the first 2 minutes and a flattening out after 5 minutes. An equation for the decay time exists and can be found in Yamamoto et al.[10]. As the samples were procured from multiple companies, a series of decay curves for green, aqua and blue were plotted. This procedure was not performed for the colors purple and red as they performed poorly during the spectral tests. The decay curves have been plotted on a log – log basis with the Log of luminance (mcd/m^2) on the y axis and the Log of time on the x axis (minutes). Figure 3-9 A shows the decay for the green powder and pebble samples. As can be seen, the slowest decay rates were reported for AGT's samples. This was the same case in Figure 3-9 B where more green samples have been compared. Small variations exist between the sizes, but it is the surface geometry and number of stones that may have been responsible. Hence, the luminance is not size dependent.

The log-log curves were also plotted for aqua and blue in Figure 3-10 A and Figure 3-10 B, respectively. AGT's samples performed the best in this case as well. To compare the effect of different colors on the luminance, Figure 3-11 serves as a reference. It is noticed that the green samples would have the longest luminance duration of all the colors which makes them a good candidate for further tests. Finally, Figure 3-12 compares an extrapolated curve for green with results in literature. A decay time of 12 hours was predicted after extrapolating to 3 mcd/m^2 (full moon on a dark street) which closely agrees with the estimation by Matsuzawa et al.[6] which is 11.5 hours. Hence, AGT's green samples serve as viable candidates for concrete and asphalt testing.

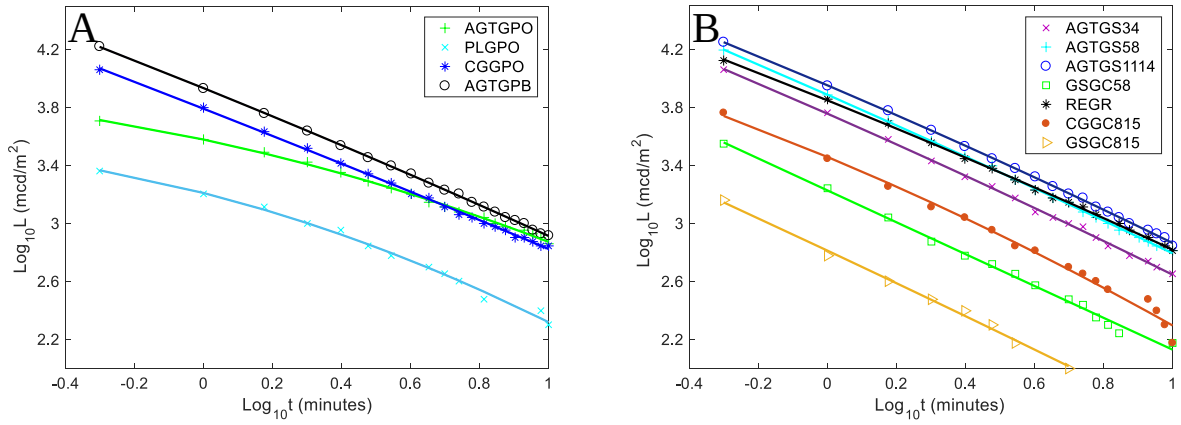

Figure 3-9. (A) Luminance decay curves for green powders and pebbles, fit through a second -order polynomial. The values on the x- and y-axes were converted to logarithmic values to compare decay rates between companies. (B) Luminance decay curves for other sample sizes. As can be noticed from this figure and the one above, Ambient Glow's and Rare Earth's samples performed the best.

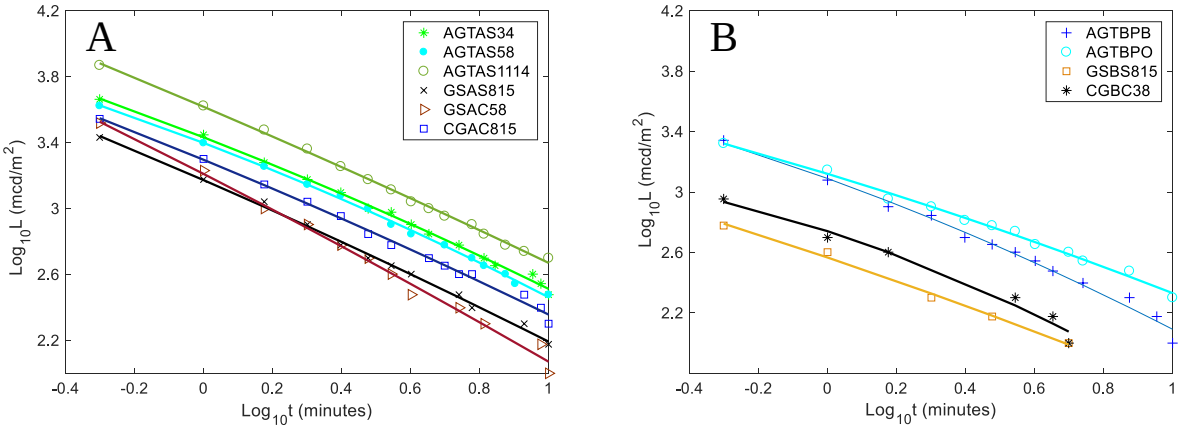

Figure 3-10. (A) Luminance decay curves for aqua samples. Notice a decrease in the luminance values when compared to the green case. (B) Luminance decay curves for blue samples

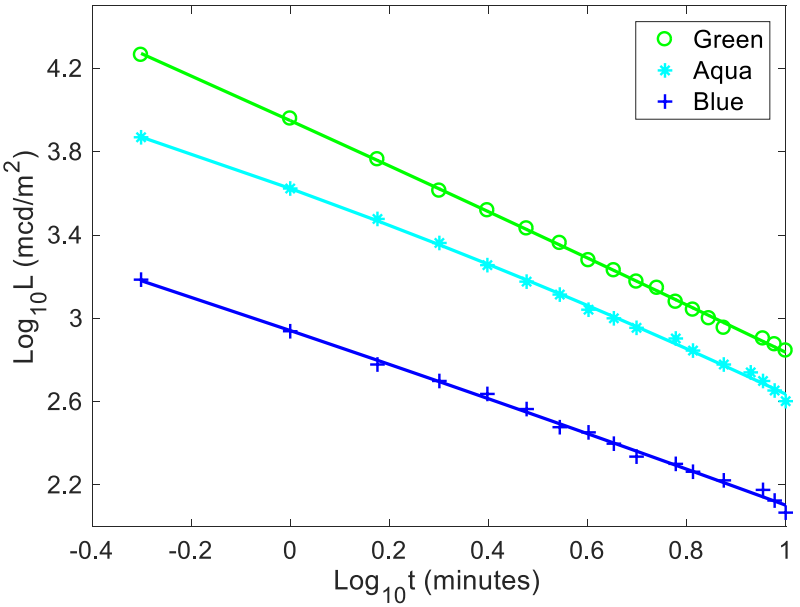

Figure 3-11. Comparison of the rate of decay between AGT's green, aqua, and blue samples

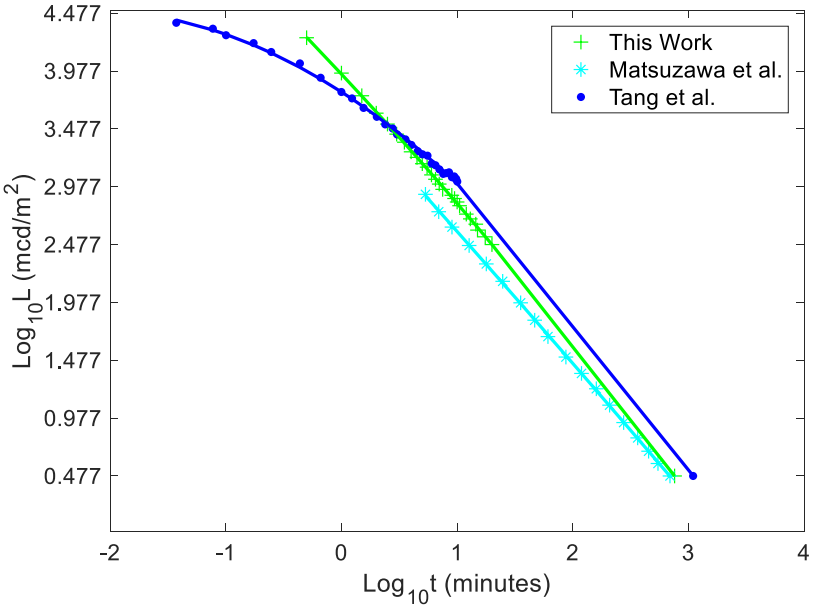

Figure 3-12. Comparison of decay curves between this work and literature. We notice that the decay time estimated by the experiments conducted in the thesis approximates the decay time from Matsuzawa et al.[6] experiments. The curve for this work was a long-term extrapolation while the curve from Matsuzawa et al. was extrapolated from a luminance of value of 3.84 mcd/m^2 to 3 mcd/m^2 (log value = 0.477), which is what we require.

Phosphor-Embedded Concrete and Asphalt Samples

The prior section discussed the impact of sample geometries and color of samples procured from a number of manufacturers on the luminance decay. Overall, for all colors, Ambient Glow's stones were the most suitable for usage in construction applications on the basis of emission peaks and the luminance curves. We also analyzed the differences in luminance between stones of different colors and determined that the color green had the highest luminance and slowest decay rate, and its emission peak was the closest to the maximum spectral sensitivity limit at 555 nm. The goal of this section is to investigate the impact of sample geometry on (1) the suitability of Ambient Glow's green stones for integration into concrete and asphalt mixtures and (2) their luminance once fabricated into laboratory-scale coupons.

Experimental Methods

All tests were performed on Ambient Glow's AGTG11114, AGTGS58, and AGTGS34 samples. The powder samples were not tested because they required an epoxy matrix as a sealant. The pebble samples were also not tested because they remained covered by the concrete after fabrication.

Concrete Fabrication

For fabricating the concrete samples, two sets of tests were performed. A concrete mix was utilized which was composed of cement, sand, and water. The objective here was to determine the best way to place the stones in the concrete mixture. The specifications for the concrete used are listed below and a detailed account on types of concrete can be found in FDOT's manual[27]. The cementitious material includes cement and any other additional materials added to it, such as fly ash.

1. Cement Type : Type I
2. Cementitious material content: 670 lb/yd^3
3. Water to cementitious material ratio : 0.40

Test Set 1 - The concrete mix was set into different dishes and was pre-cured for 5 minutes to allow it to slightly harden. The top surface of concrete was flattened using a putty knife. Stones of various sizes were then sprinkled on top of the concrete layer. These were the 3-4 mm, 11-14 mm, and powder samples. The glow color was not fixed for this test because it was performed in conjunction with the color comparison tests discussed in the prior section. The dishes were then placed on a vibrating table, which allowed the stones to set into the concrete. Figure 3-13 shows the table with some dishes on the top. Powder samples were not used for Test Set 1 because they require an epoxy sealant for stability in the mix. Hence, only stones

Figure 3-13. Flattened concrete samples placed on a vibrating table. The vibration allows the stones to set into the mix.

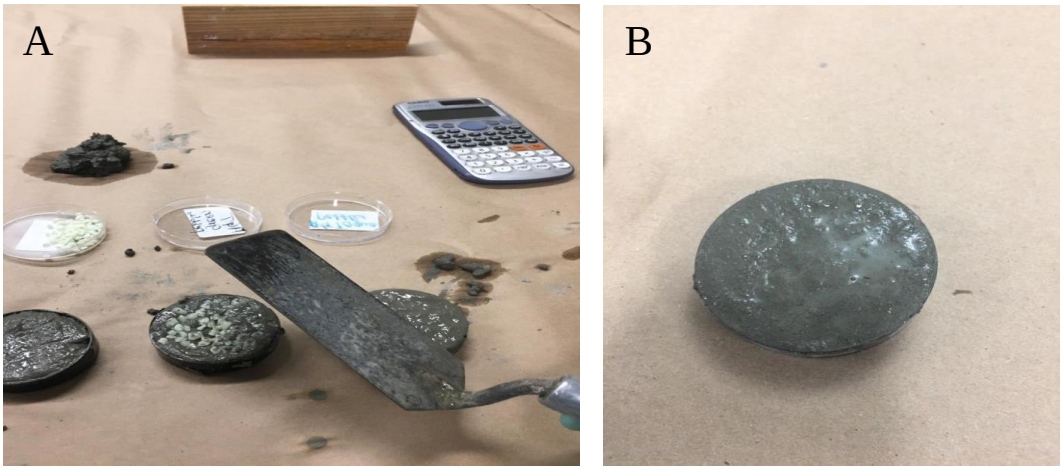

Figure 3-14. Experimental steps for stone placement: (A) Applying stones and smoothing with a trowel and (B) after retarder applied on the surface.

were used for Test Set 1 because they do not require additional stabilizing agents.

Test Set 2 - 9 petri dishes were selected, 3 for each size with the sample sizes again being the same as for the previous test case. The masses of all the samples was kept roughly the same and around 2500 mg. This allowed us to compare results between different sized aggregates. Here, a concrete retarder was used instead of a vibrating table, the purpose of which is to expose the photoluminescent samples. The retarder application and testing procedures are similar to the ones suggested by Ambient Glow (https://ambientglowtechnology.com/pages/how-to-apply-agt-professional-grade-glow-stone).

A series of steps below outlines the process. Figure 3-14 shows a series of pictures depicting the process followed. In the first step, the concrete mix was placed in placed in 9 petri dishes as discussed above. The mixes were placed in the dishes at about the same time with a 5 minute difference between the first and last placing. Water was added to mixes in which pressing the stones in was difficult. The mixes were then allowed to pre-cure for 5 minutes. Following the above step, the stones were sprinkled onto the concrete surface as in Figure 3-14 A. They were then worked under the top layer by the means of a putty knife. This procedure is similar to the usage of a trowel for large scale applications. The whole process took about 10 minutes. A thin layer covered the surface of the stones which also allowed the stones to be felt at the top. Care was taken to ensure that the stones did not sink into the mix as the application of a retarder in the next step requires a thin layer.

A retarder is a chemical agent which is used to expose the aggregates at the top surface of concrete. It works to un-cure the top layer of concrete while the bottom layers continue curing. Its application also allows the below aggregates to settle down normally into the mix by gravity. For this concrete experiments, a sugar-water retarder was used containing 4 parts of water by 1 part of sugar on a volume basis. The retarder was applied as soon as the stones were applied (Figure 3-14 B).These were then kept covered for a period of 24 hours.

Finally, after 24 hours, the mixes were uncovered by peeling of the top layer with a wet brush. The final result is shown in Figure 3-15. The figure also shows the side view of mixes made with two different stone sizes. This was done to compare the setting of different sized samples in the

mix. Complete curing of all samples took seven days, during which they were covered with a wet towel to provide moisture.

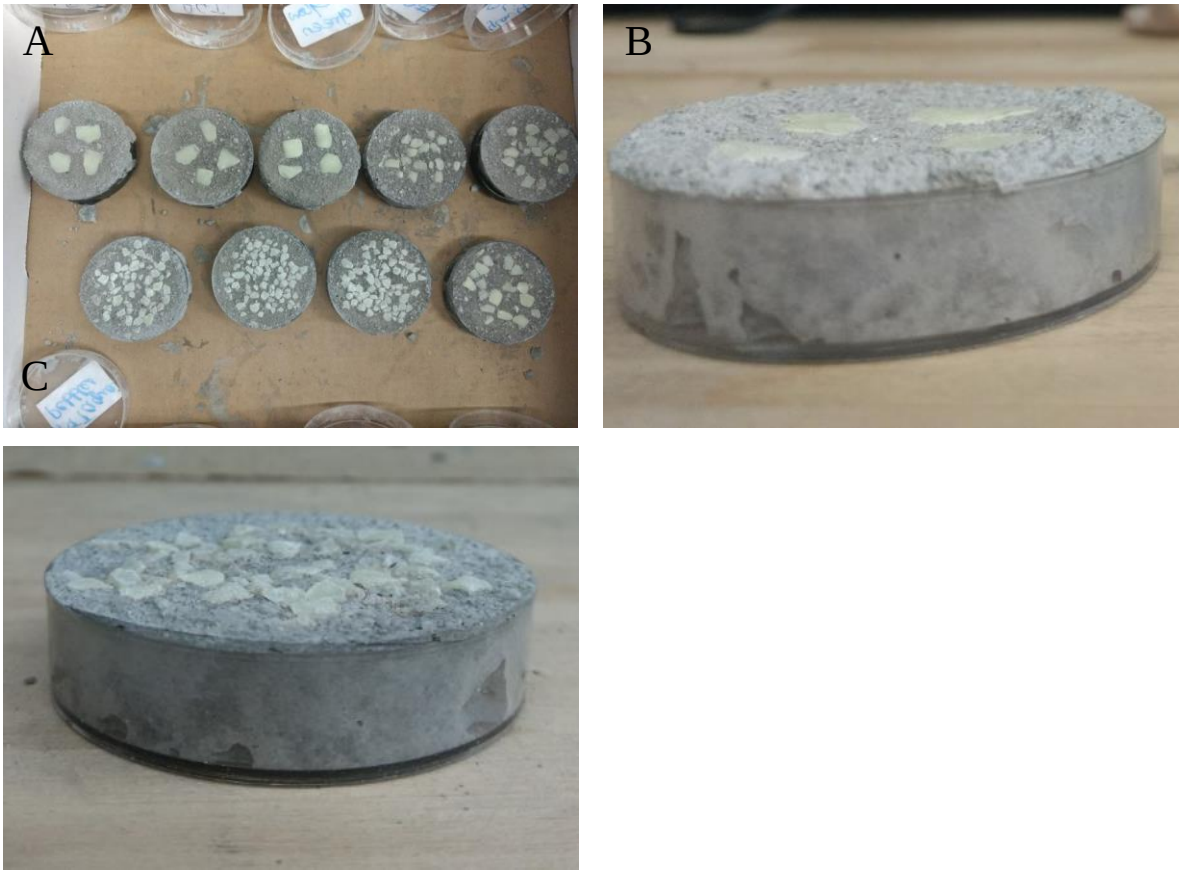

Figure 3-15. Retarder testing stages for the concrete sample: (A) Samples uncovered after 48 hours, (B) and (C) Samples compared for their flatness.

Figure 3-16. Compacted asphalt cylinder. Going in a clockwise manner, notice the 11- to 14-mm, 5- to 8-mm and 3- to 4- mm stones.

Asphalt Fabrication

Asphalt fabrication was done through the usage of a black hot asphalt mix. The mix was introduced in a cylinder to form a cylindrical mold. The mix was at a temperature of 300 º F which is the compaction temperature. Compaction is a process in which air voids within the asphalt mix are closed up to make the material strong. This is usually accomplished through rollers[28].The mold was partially compacted before the introduction of the photoluminescent stones. Full compaction took place thereafter through gyrations in a Superpave Gyratory Compactor. The Gyration number tells us the effort during compaction and the number of rotations made for setting the mix. Once the mixture was set it was allowed to cool down to obtain an asphalt cylinder as

in Figure 3-16. All three stones were placed in the single mix. This is contrast to the case in concrete where a single mix was reserved for only one stone size due to the small nature of the samples.

Results and Discussion

Concrete Fabrication

Looking at Figure 3-17 A and B for Test Set 1, it is apparent that that larger stones are sticking out of the mix and smaller stones tended to settle more. This disparity was caused by the vibration table as the vibration process cannot easily control the depth of immersion of the stones.

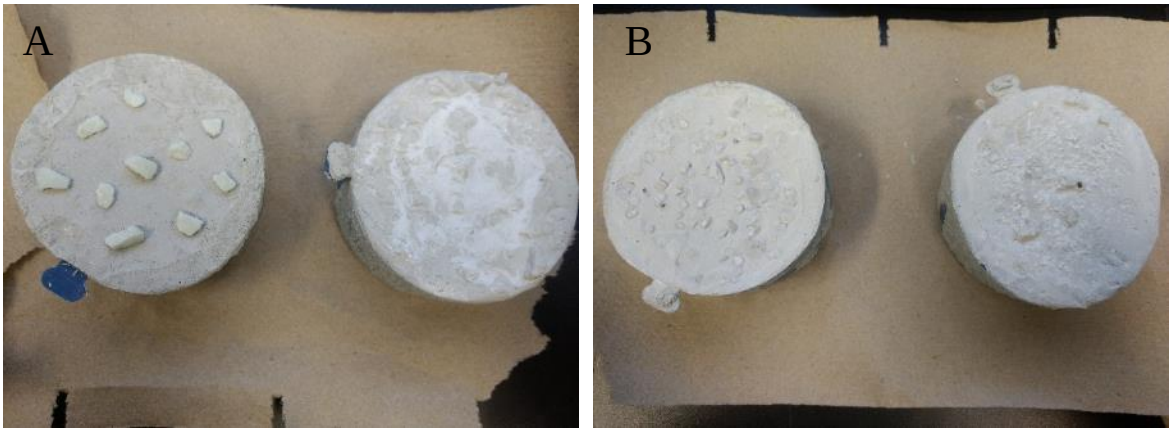

Figure 3-17. Results of vibrating table tests: (A) Stones sticking out and covered portions of applied powder, to the right, (B) Stones sitting overexposed in the left and pebbles covered with concrete to the right.

In Test Set 2 a retarder was used as described above. After the top layers of the mixes were uncovered using a brush, it was noticed that the stones sat in flat at the top. This was the case for all the samples that were made. Figure 3-15 shows the results after 48 hours had passed after the testing day. Figure 3-15 also shows the results of 2 fully cured samples containing 11-14 mm and 3-4 mm stones. The side view in Figure 3-15 B shows the 11-14 mm samples sitting flat at the top while it is noticed that the 3-4 mm stones formed a jagged surface due to them sticking out (Figure 3-15 C). The same was observed for 5-8 mm stones. Their small sizes made it difficult to place them more easily in the mix. Further, a few of them got dislodged while the retarder was removed. On the other hand, the 11-14 mm stones bonded well with the mix and had no issues. The smaller stones also got covered by the concrete in some areas. Hence, it may the best to use the largest stones when laying the concrete sidewalk.

Figure 3-18. Cracked stones as a result of their large size and the compaction process.

Asphalt Fabrication

As seen in Figure 3-18 it is apparent that the 11-14 mm stones cracked after the high compressive forces during the compaction process. This was cause due to the compaction process where these stones were too large to be forced into the voids. The smallest stones experience a different issue wherein, they did not sit in the voids properly as they were too small to bind

themselves to the mix. A few of them also got dislodged and covered by the asphalt as a result. No issues were experienced with the 5-8 mm stones and hence they may serve the best option for the asphalt bikeway.

Afterglow Behavior of Embedded Concrete and Asphalt Mixtures

Luminance measurements have been performed on concrete samples to try and determine the effect of sample particle size integrated into the concrete on the luminance decay. Further, we have used time lapse photography to visual observe the decay of both concrete and asphalt mixtures.

Experimental Methods

Luminance Measurements

As the stones were spread randomly in the concrete samples, there is a need to couple the light emitted from them for making luminance measurements, due the probe's narrow measuring angle of 2 degrees. This was accomplished through the additional of 2 lenses to the setup. An aspherical lens (Diameter = 75 mm) kept above the sample collimates the light while a plano convex lens (Diameter= 50 mm) above it focuses the light into the detector. The orientation of the lenses and the distances between them and the detector were fixed by the means of a red laser pointer. The modified portions of the setup have been shown in Figure 4-1. The experimental steps followed for making measurements are as follows:

1. All samples were discharged for at least 24 hours as was done prior.
2. The LED was used for an illumination period of 20 minutes.
3. Data was recorded a minute after end of excitation which allowed time for positioning of the samples under the lenses.
4. Readings were acquired for the short time period of 10 minutes.
5. All samples were clearly marked for identifying possible differences in luminance between samples having similar sized stones.

Time-Lapse Photography Measurements

Prior we used extrapolation techniques to predict the theoretical decay time. This was also corroborated by different authors. However, the extrapolation serves as an estimation technique. To get a visual picture of the decay, time lapse measurements can prove very useful. For achieving this, a time lapse camera was utilized. The following experimental procedure was used:

1. As in the luminance test, samples were discharged for 24 hours and were illuminated for 20 minutes. In the case of concrete, the 11-14 mm sample was illuminated while for asphalt the 3-4 mm was illuminated as they could fit the LED beam's spot size.
2. A time lapse camera was then set inside the enclosure to record the decay over a period of 12 hours, every minute.
3. The data was then acquired and then analyzed on the basis of time stamps which were present at the bottom of the captured shots.

Results and Discussion

Luminance Measurements

The luminance results for all the tested samples is depicted in Figure 3-19. We see that the 11-14 mm samples, which were three in number, performed the best in that they started out with the highest value of luminance and reported the slowest rate of decay. These performed well as they sat flat at the top and they were distributed evenly around the dish. The stones were also not in close contact to allow radiation exchange. Further, the least of amount of concrete covering their surface also helped along with the stones being distributed within a diameter of 40 mm. The 40 mm diameter works as the maximum diameter within which the plano- convex lens can efficiently focus light. Hence, as a result coupling the light from these stones through the optics and into the detector led to higher values.

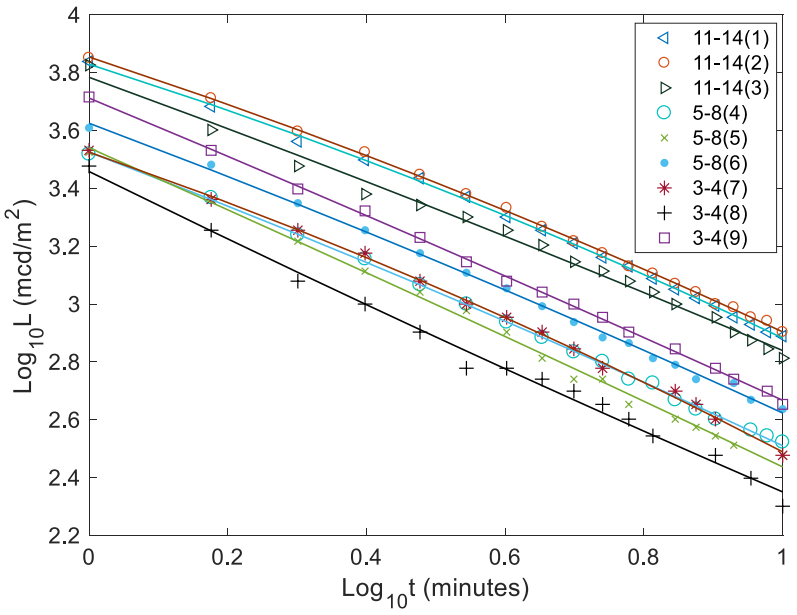

Figure 3-19. The luminance curves for nine samples made. As can be seen, the 11- to 14-mm aggregates gave the best results after the optical testing.

For the smaller sized stones, their scattering towards the edges of the petri dishes reduced luminance values as they were beyond the tolerance limit of 40 mm, as discussed above. The tolerance limit also posed a problem in illumination as the LED spot size was also about 40 mm and hence some areas did not receive light at all. Further, they were closer to each other which allowed radiation exchange. Finally concrete covering their surfaces also caused a reduction in luminance values. These effects were more pronounced for the 3-4 mm ones which explains why they performed more poorly than the 5-8 mm ones.

Time-Lapse Photography Measurements

Time lapse images of the concrete composite is shown in Figure 3-20. The decay is rapid for the first 1 hour with it being slower thereafter. By the end of 12 hours the stones can still be seen, though the glow is very faint. Visually, the stones may seem as bright as a street with moonlight shining on it and with no cars or auxiliary lights around. The luminance value for such a situation is around 3 mcd/m^2 which is what was addressed prior. Hence the extrapolation model does give us an estimate.

In the case of asphalt, the glow was again observed for around 12 hours as seen in Figure 3-21. Here though the sample seemed to glow less faintly at the end as compared to its concrete counterpart. This happened as a result of asphalt's higher absorptivity. Certain portions of the stones were facing the black surface while some were slightly below the top surface. This led to light absorption and hence a reduction in the glow observed after 12 hours.

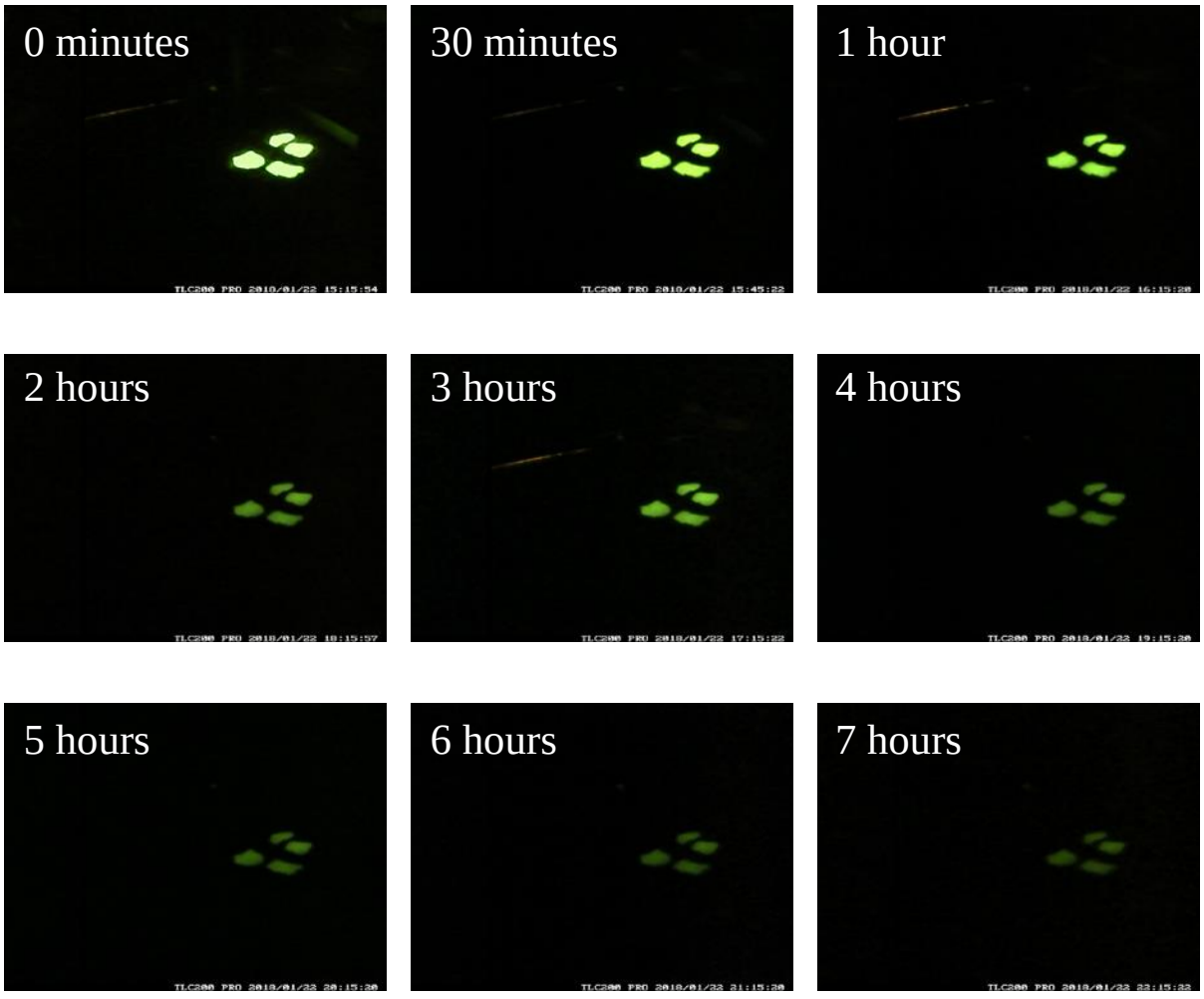

Figure continued on next page

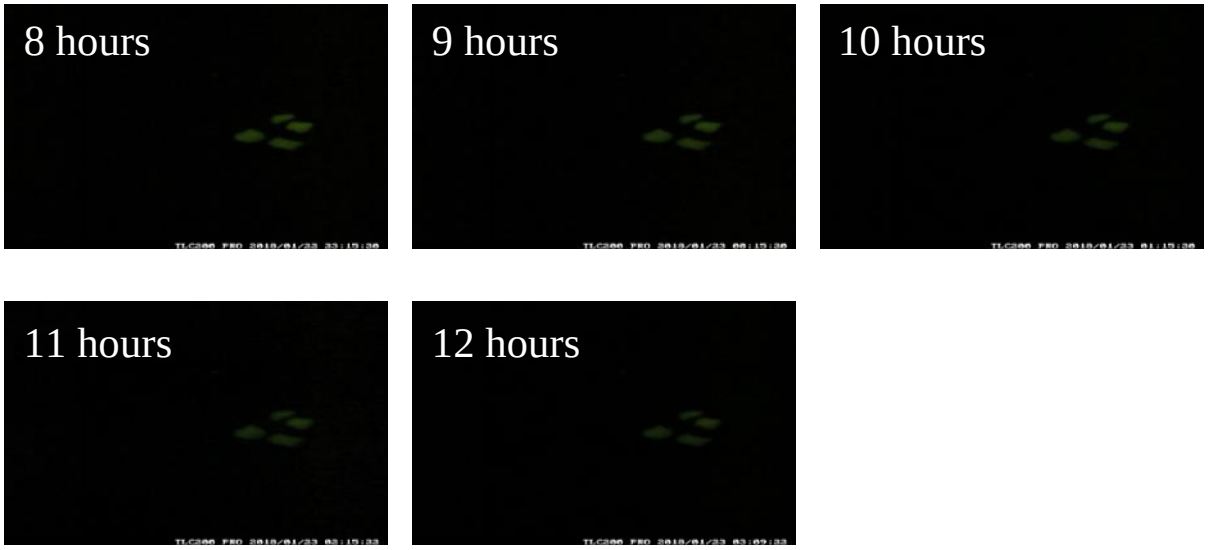

Figure 3-20. Afterglow pictures for concrete. The time stamps have been written at the bottom of each of the figures. We notice that the decay is fairly rapid for the first 2 hours with it being slow thereafter until the12-hour limit is reached. The stones are still faintly visible after 12 hours.

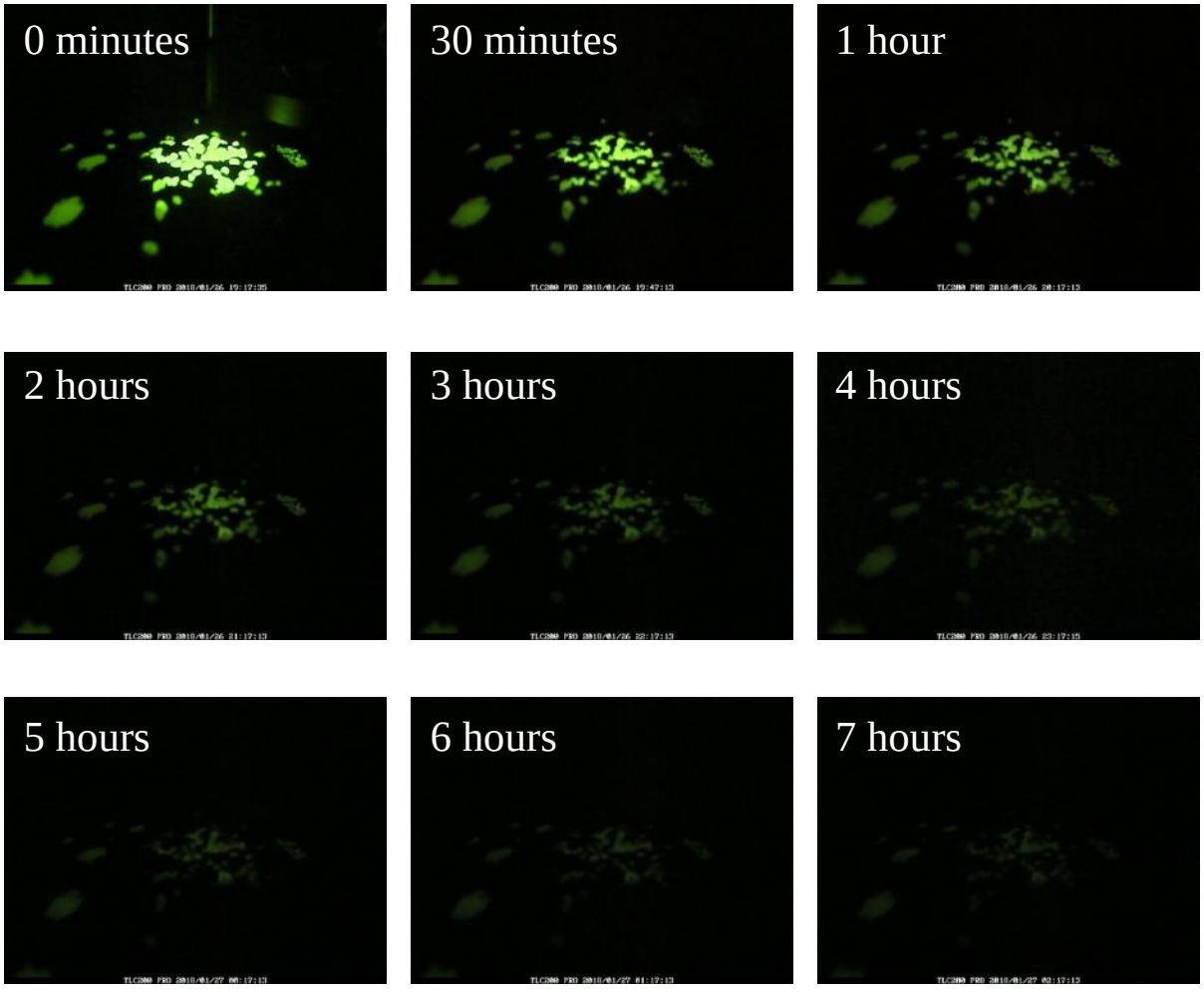

Figure continued on next page

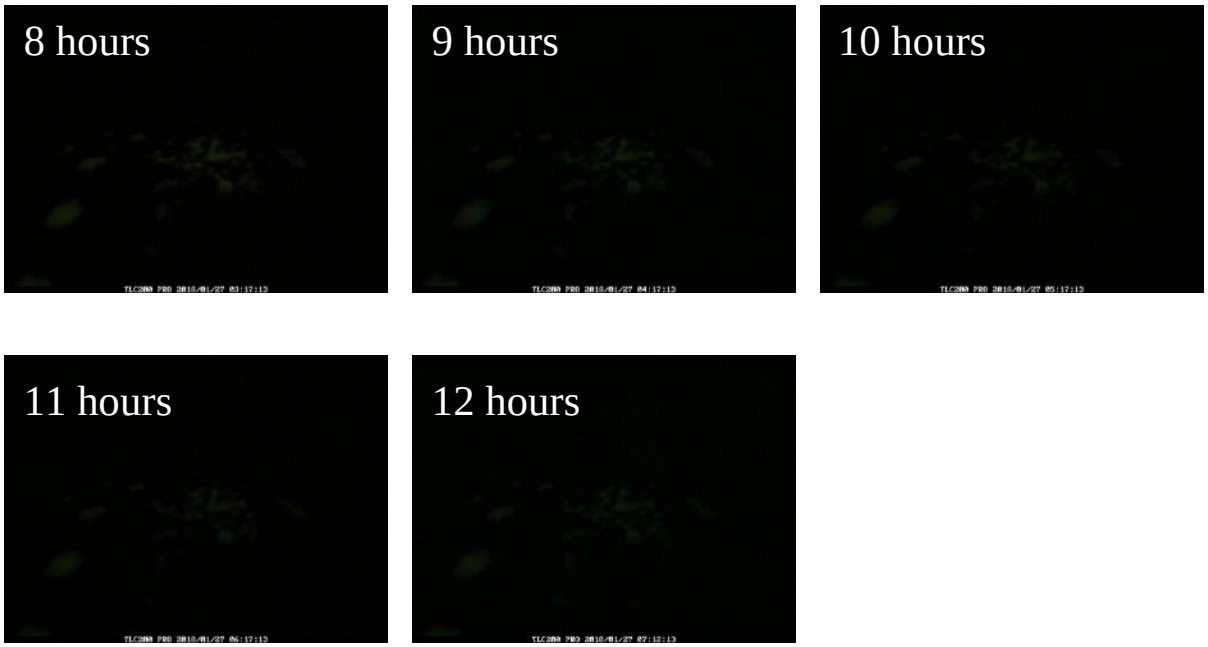

Figure 3-21. Afterglow pictures for asphalt. The pictures resemble a mini-walkway with the stones visible ahead at a distance. We can also see that these are fainter by the end of 12 hours as compared to the concrete samples.

Chapter 4 **Stones in Concrete and Stones in Asphalt Installations at TERL**

Description of Site Visit on 3/2/18 and Determination of Installation Locations

On March 2, 2018, the UF team visited the Florida Department of Transportation Traffic and Engineering Research Laboratory in Tallahassee to determine installation locations for the photoluminescent asphalt roadway and the concrete sidewalk. Pathway locations are depicted in Figure 4-1. The proposed concrete section (blue) would connect to an existing concrete pathway and would be 149-ft long by 5-ft wide. This section would curve along the roadway from the traffic signal to the barrier (see Figure 4-2). The pathway would be entirely in the sun with no shade.

The asphalt section would connect two existing roads at the FDOT site. It would be placed

Figure 4-1. Satellite view of TERL facility with proposed pathways.

across a field to be used as a road for buses that are currently parking in that location. There were two suggested pathways for the asphalt section: the first one was 247-ft long (yellow), and the second was 288-ft long (orange). Both pathways would start and end at the same location. The first proposed section would receive both road and pedestrian traffic and was in an area with sun and shade to provide a wide range of environmental conditions. The second proposed section would be entirely in the sun.

The final chosen path for the roadway was the 247-ft path (yellow) because it offered the most direct route across the field and would be simplest to pave. Images of the beginning and ending of the pathway are shown in Figure 4-3.

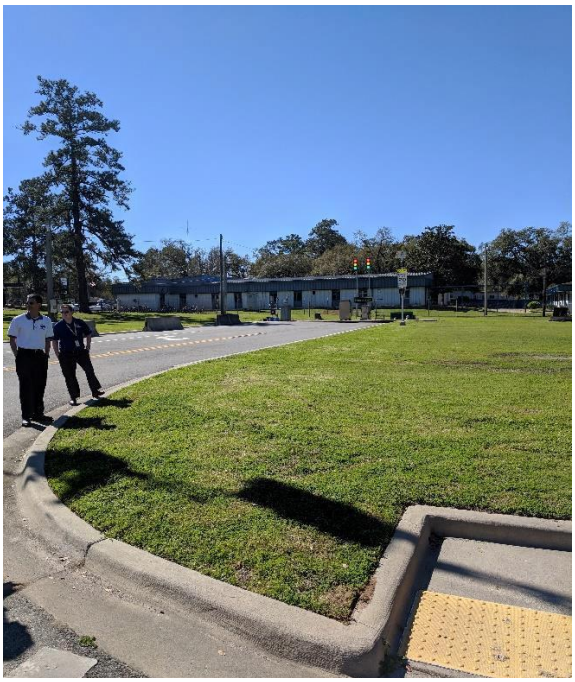

Figure 4-2. Concrete section will connect to existing sidewalk at lower right and extend to barrier at the end of the roadway.

Figure 4-3. Beginning of both proposed asphalt sections (left) and end of both proposed asphalt sections (right).

Contractors

Multiple concrete and asphalt contractors in the Tallahassee area were contacted and here are the quotations received:

Table 2. Potential contractors for concrete and asphalt installation

Company	**Contact Number**	**Contact Name**	**FDOT TERL Site Visit Date**	**Concrete Quote**	**Asphalt Quote**
North Florida Asphalt	850-792-8431	Kathy Shirah	4/3/2018	$6,750.00	$17,775.00
All Star Asphalt & Concrete Repairs	850-363-1834	Daniel Smith	3/28/2018	$6,350.00	$9,000.00
Thomas Concrete & Construction Services	850-528-7543	Brandon Thomas	3/29/2018	$3,250.00	N/A
North Florida Concrete Coatings and Countertops	850-529-5612	Travis Barlar	3/27/2018	$4,000.00	N/A

Each contractor was asked to visit the construction site at FDOT's Traffic Engineering Research Lab (TERL) to provide accurate cost estimates and installation procedures. North Florida Concrete Coatings and Countertops was recommended to us by several other concrete contractors in the area and was ultimately selected for the concrete installation. The owner, Travis Barlar, provided helpful insight on how to best integrate the stones into the concrete based on his prior experience in installing decorative concrete.

Finding a contractor in the Tallahassee area to install the asphalt path proved to be more difficult, and only two quotations were received. All Star Asphalt & Concrete Repairs was also recommended to us for custom projects and was ultimately chosen for the asphalt installation.

Development of Monitoring Stations for Installations

Three electronic enclosures were designed and installed on sight. The purpose of these enclosures is to measure the global horizontal solar irradiance, temperature, rain, time lapse photography and luminance during the night. Each enclosure contains two remotely operated computers for automatic data acquisition that is uploaded to the cloud for analysis from Gainesville, FL. The concrete installation has a single enclosure monitoring it because it is installed completely in the sun. The asphalt installation has two enclosures monitoring it because it has sunny and shady areas to observe.

Hardware Description

The instrument enclosures we used to house all the sensors and hardware was provided by Omega Engineering. We used a non-metallic fiber glass with a transparent polycarbonate cover, as shown in Figure 4-4. The enclosure type guaranteed that the equipment inside will be protected against solids, liquids, and the formation of ice, if needed. We acquired three

enclosures with dimensions of 16” H x 14”W x 8” D, to monitor three different portions of the installations, two in the asphalt section and one in the concrete. The objective was to come up with monitoring stations that will take up data from a luminance meter, time-lapse camera, pyranometer, temperature sensor, etc.

Each enclosure is unique but the common instruments contained within each are:

- One luminance meter
- One camera tripod, used to support the luminance meter
- One Raspberry Pi 3+
- One Raspberry Pi 3+ camera with pan/tilt system
- One Arduino Uno R3
- One temperature and relative humidity sensor
- One mini PC
- One Ethernet switch
- One power distribution terminal block
- One 12V power module
- One 5V power module

Figure 4-4. Fiberglass instrument enclosure without modifications.

The luminance meter (Konica Minolta, Luminance Meter LS-150) is used to measure the luminance of the installation during the night. It was attached in the bottom to a camera tripod that allowed easy adjustments and alignment of the luminance meter into the right direction. Furthermore, the hole on the mounting table (described later) gave enough clearance for the luminance meter to fit through and be adjusted as needed.

The Raspberry Pi 3+ and its respective camera are used to take time-lapse pictures of the location. Advantages of using this instrument will be discussed in the Software description section. Moreover, they were locked in place with double-sided tape.

The Arduino Uno R3 is used in partnership with a temperature and humidity sensor. The sensor was coded and connected to the Arduino in such a way that could take measurements from inside

the enclosure at any desired time. In a similar way, the Arduino was connected and powered to the Raspberry Pi 3+, and everything locked in place with double-sided tape.

The mini PC has the same function of the Raspberry Pi 3+, but provides the advantage of having Windows installed as operating system. The different OS gave us more flexibility when installing luminance and pyranometer software and connecting them to different sensors.

The Ethernet switch is used to distribute internet connection via Ethernet to all the components inside the enclosure. The mini PC and the Ethernet switch were placed in the lower level of the enclosure with an additional aluminum sheet metal mounting table in between them. Both of them were locked in place with double-sided tape.

The initial design was built using SolidWorks and a rendering is shown below in Figure 4-5. The left side is a ventilation system that was installed to prevent overheating after some preliminary temperature and humidity tests inside the enclosure. The far right side is the proposed installed design where the enclosure is placed into concrete foundations. This allows the enclosures to be modular in a sense and thus they can be moved on sight where desired as long as power and data exists.

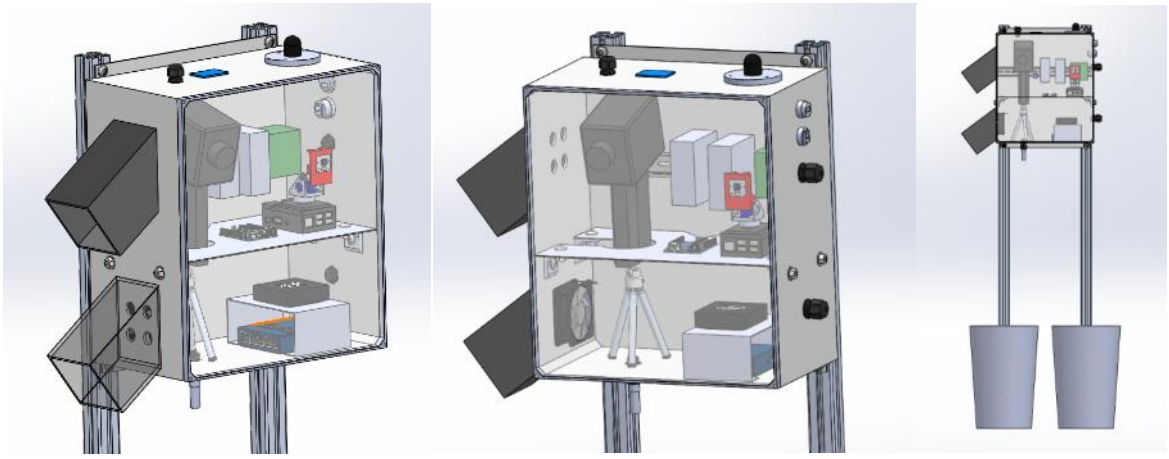

Figure 4-5. 3D model of the enclosure created in SolidWorks.

A description of the manufacturing and construction is detailed below. The first step in the modification of these enclosures was to determine which holes had to be drilled in which enclosures for the installation of the equipment inside of them because some enclosures have additional sensors and/or jobs than the default listed above (discussed below). We determined that each enclosure had to have the following holes drilled:

- Four 5/16” holes to support an aluminum mounting table, two on each side
- One 13/16” hole for the power cable, on the right side
- One 15/16” hole for the Ethernet cable, on the right side
- Three 1/4” holes for the DIN rail installation, on the back
- One 1/2” hole for the rubber plug, on the back
- Eight 13/16” holes for the ventilation system, four on the top left side and four on the bottom left one

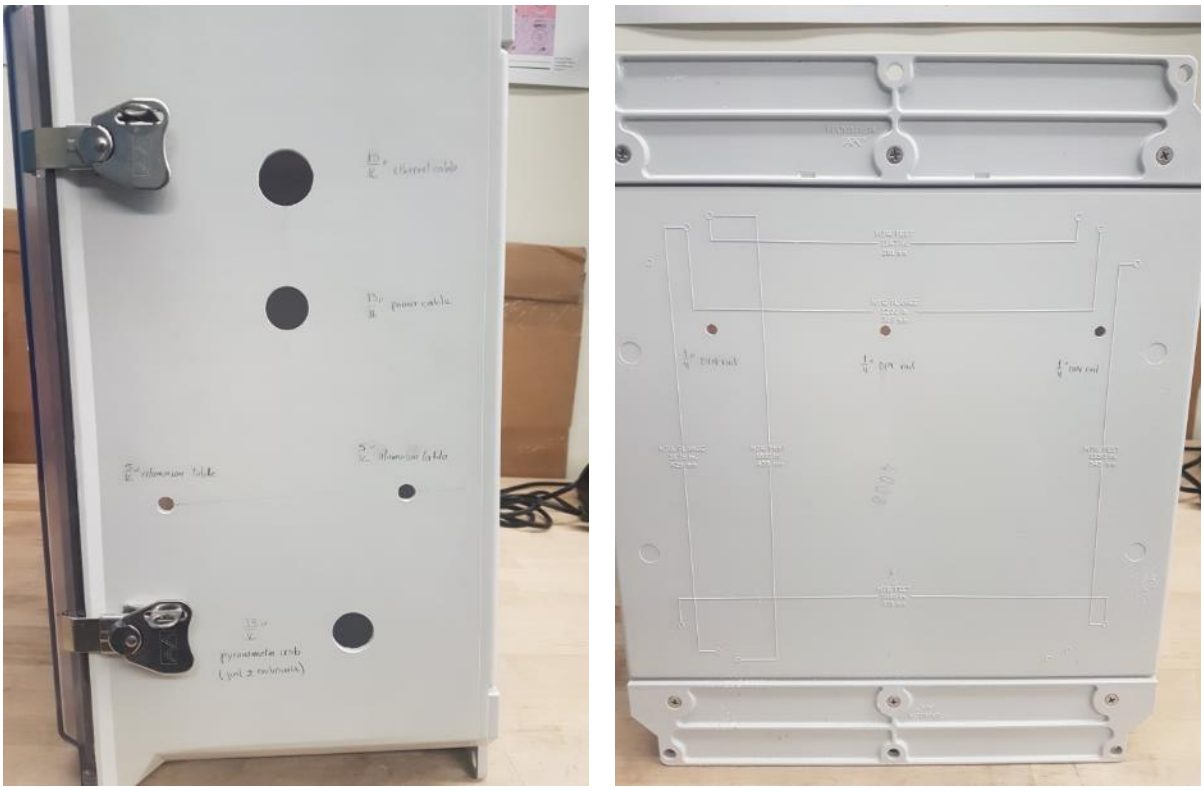

Figure 4-6. Holes drilled on the right side of the enclosure (left) and holes drilled on the back side of the enclosure (right).

A picture of the side and back of the enclosures is shown in Figure 4-6. The side holes are primarily for data and power access and the back for mounting purposes. An 18 gauge aluminum mounting table was installed to provide an additional platform to set equipment inside of the enclosure (Figure 4-7). The height at which the mounting table was placed was approximately 6” from the bottom surface. Four 5/16” holes had to be drilled to secure the table in position. A triangular cut was made on the back to allow cable connection in between upper and lower level of the enclosure. Finally, an elliptical cut was made on the left side of it to allow the installation of the luminance meter, which will be described later.

Figure 4-7. 18-gauge aluminum table.

We acquired strain relief liquid-tight connectors for cables entering and leaving the enclosure. The two holes needed for these connectors were a 13/16” hole for the power cable and a 15/16” hole for the Ethernet cable. These modifications were made to guarantee that the 4X safety standard of the enclosure won’t be compromised. In addition to the aluminum mounting table, an aluminum DIN rail was installed in the top back portion of the enclosure for quick installation of different instruments. Three 1/4” holes were made, equally spaced, to support the DIN rail on the back. The height at which it was placed was approximately 5” from the top surface. The strain relief liquid-tight connectors and DIN mounting installation is shown in Figure 4-8. A 1/2” hole filled with rubber plug in the back was installed in order to perform luminance meter alignment.

For the ventilation system, four holes were drilled in a square pattern, and were placed in the top and bottom side to guarantee an air flow across the whole enclosure as seen in Figure 4-9. The air flow was powered by a 4” x 4” computer fan installed on the intake side of the ventilation. To guarantee weather-proof protection of the enclosure, filter paper was installed on the intake and outtake, and PVC pipe was placed diagonally on the outside.

Figure 4-8. Strain relief liquid-tight connectors (left) and DIN rail mounted on the back side of the enclosure (right).

Figure 4-9. Ventilation system. Intake and exhaust with filter paper and powered by a computer fan. PVC pipe placed diagonally on the outside of the enclosure.

The power distribution terminal block (Figure 4-10) was used to distributive power from the grid to all the instruments inside the enclosure. This was used to provide power to a 12V power module, a 5V power module, and a 9V converter. All these instruments were mounted on the DIN rail on the back of the enclosure.

Each enclosure had all of these basic instruments and connections made. However, depending on the location and function, additional sensors were installed to each enclosure differently. The specifications of each enclosure are as following:

Enclosure 1

Figure 4-10. Power distribution block connected with power modules and converter (left). Connections mounted on DIN rail (right).

The only additional modification made to this enclosure was an Ethernet output connection. Enclosure 1 will receive Ethernet and will distribute it via the switch and pass it to Enclosure 3. One 15/16” hole had to be drilled on the bottom right side of the enclosure for strain relief liquid-tight cord connector to be placed.

Enclosure 2

This enclosure contains the most equipment. It included a pyranometer sensor (Apogee instruments SP-420) on the top, which is used to measure the irradiance of the sun. Three 3/16”

Figure 4-11. Three 3/16” holes for pyranometer attachment (left). Pyranometer locked in place and connected to Mini PC via USB cable (center). Raindrop sensor and outdoor temperature and humidity sensor connected to Arduino (right).

holes had to be drilled on the top, and the pyranometer with its base was securely attached. It was connected via USB to the mini PC so an additional 13/16” hole was drilled on the bottom right side of the enclosure (Figure 4-11). Two additional sensors were installed in this enclosure, a raindrop sensor and an outdoor temperature and humidity sensor. Both of these were coded and connected to the Arduino. The raindrop sensor required a 1/2” hole drilled on the top of the enclosure coupled with a strain relief liquid-tight cord grip connector. The outdoor temperature and humidity sensor required another 1/2” hole drilled on the bottom of the enclosure.

Enclosure 3

This enclosure’s only modification was the addition of a pyranometer on the top. We decided to also include a pyranometer on this enclosure because it measures data in a shaded region rather than one that is completely sunny like Enclosure 2.

Initial Set Up

Once on site, all of the final connections were made. The Raspberry Pi, its camera, the Arduino with its sensors, and the mini PC with the switch were fixed in place with double-sided tape. The luminance meter was screwed into the camera tripod; it was aligned, and fixed in place (Figure 4-12). To guarantee that the enclosure will stay fixed in place, it was attached to two 80/20 aluminum extrusions on the back, which were secured in two buckets filled with concrete. For

additional safety, all the cables coming in and out of the enclosure were attached with a strain relief loop to the 80/20 extrusion. Finally, a 10’ strap secured each enclosure to the ground while attach to two 1’ ground anchors (Figure 4-13). The final locations of the enclosures installed on sight can be seen in Figure 4-14 below.

Figure 4-12. Final design on site without (left) and with luminance meter (right)

Figure 4-13. Enclosure set up with 80/20 extrusions and secured to the ground.

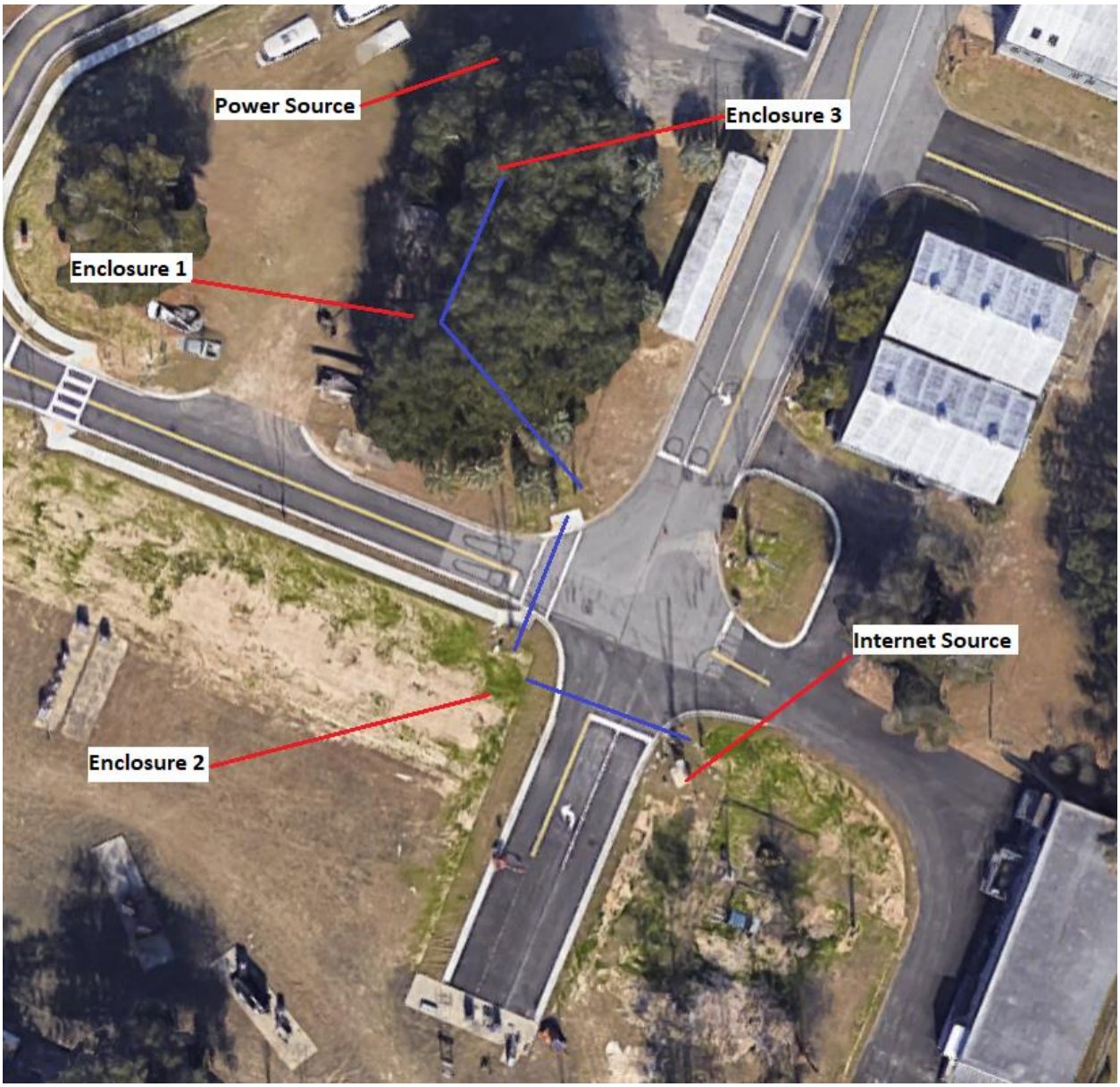

Figure 4-14. Location of enclosures on map. Blue lines denote Ethernet cables.

Software Description

For this project there are three sensor stations, with each station housing its sensors in an enclosure. There are two main subsystems per station: a miniature Microsoft Windows computer and a Raspberry Pi development board. All of the files were stored on the University of Florida's Dropbox system due to the nearly unlimited size that it allows us to use.

The miniature computer subsystem was used to collect data from each enclosure's luminance meter and from the two pyranometers, with one station not having a pyranometer. The miniature computers use software from the sensor manufacturers to communicate with and log the sensor data every five minutes. The Dropbox sync utility was then used to sync and store the data remotely to our private folder.

The Raspberry Pi development board subsystem worked in conjunction with an Arduino Uno microcontroller to log time-lapse photos and secondary sensor information. The sensor data and time-lapse photos were updated every five minutes. The Raspberry Pi used custom code to take a photo of the installation in front of the enclosure. The Raspberry Pi used the Raspberry Pi Camera v2, which was made specifically for the Raspberry Pi, and allows for 4K photos. These photos are dated and numbered throughout the day and saved as 4K-resolution JPG files.

The Raspberry Pi interacted with the Arduino Uno via serial USB communication through custom code. The Arduino Uno had various sensors attached to it, and all sensor data were relayed back to the Raspberry Pi. At most, the Arduino Uno had the following sensors attached to it: raindrop sensor, external temperature and humidity sensor, and internal temperature and humidity sensor. Only one station had all three of these sensors, while the other two enclosures only had the interior temperature and humidity sensor. The raindrop sensor returned a value of 0-1023, with 0 meaning heavy rain. The two types of temperature and humidity sensors both measured temperature in Celsius and humidity as relative humidity. The external temperature and humidity sensor used a waterproof sensor to monitor the environment outside the enclosure, while the internal sensor monitored the interior conditions of the enclosure. The internal sensor was used to make sure that the interior conditions did not exceed the maximum tolerances of any component.

The Raspberry Pi used custom BASH and Arduino code to save all of the sensor data as a CSV, a spreadsheet file. The Raspberry Pi then used a Linux-variant of the Dropbox sync utility to back up and save the CSV and time-lapse files. Other custom BASH scripts on the Raspberry Pi allowed it to create and maintain storage space.

Installation

Based on performance discussed in the prior chapter, we decided to use ½" green stones for the concrete installation and ¼" green stones for the asphalt, both from Ambient Glow Technology. Samples were delivered in 1-lb bags, and we then spaced these appropriately for each installation. For the concrete, we placed one bag every 5 feet. The area was 5 feet x 7.4 feet, or 37 ft^2, and the average number of stones per 1-lb bag was 370. Thus the density of stones used was 10 stones per ft^2. For the asphalt we placed one bag every 8 feet for the first half of the installation and two bags every 8 feet for the second half. The area was 8 feet x 4 feet, or 32 ft^2, and thus, the average number of stones per 1-lb bag was 287. Thus, the density of stones used was 9 stones per ft^2 and 18 stones per ft^2.

Concrete Installation

For the concrete, stones were dispersed about 15 minutes after it was poured and smoothed, and then the contractor smoothed the surface with a trowel. A retardant sugar based solution was then sprayed over the concrete surface to prevent curing, and about 5 hours later the contractor washed away the uncured surface to reveal the stones. A pictorial summary of the process is shown below.

The site was first prepared and leveled as shown in Figure 4-15 below.

Figure 4-15. Site leveling and preparation for concrete installation

Following that, on the morning of June 8th, the concrete was poured and then leveled as seen in Figure 4-16.

Figure 4-16. Concrete installation immediately following concrete pour and smoothing

Figure 4-17. Sprinkling stones, followed by smoothing with a trowel (left) and spraying a retardant solution on the top, smoothed surface (right).

About 15 minutes after the concrete was allowed to settle, the photoluminescent stones were sprinkled into the wet concrete by hand as seen on the left side of Figure 4-17. To test if the time was sufficient a few stones were dropped into the wet concrete to make sure they did not sink below the surface. Immediately after sprinkling the stones, the surface was smoothed with a trowel to cover the stones. Immediately following smoothing, a pressure sprayer was utilized to spray a fine layer of sugar based retardant as seen on the right side of Figure 4-17. This was repeated 4 times to ensure complete retardant coverage.

Figure 4-18. Top surface is washed away after 5 hours, revealing the exposed surface and glowing stones.

About 5 hours after the retardant was applied, the contractor returned to wash or rinse away residue on surface, resulting in the exposed surface as shown in Figure 4-18. At the top side of the image the water leaving the hose nozzle can be observed and the granular substance from the top surface being washed away.

The concrete installation was then cured overnight and then cut into 5 ft sections to relieve stresses. Final, installed pictures are shown below in Figure 4-19. As seen, the stones are well integrated into the concrete and the surface is exposed.

Figure 4-19. Pictures of the final concrete installation (top) and a zoomed-in image showing the exposed surface with glowing stones well integrated (bottom).

Asphalt Installation

During asphalt installation, the stones were, for the most part, dispersed immediately prior to rolling the hot asphalt. However, in some instances there were miscommunications with the contractor that caused the roller to pass over the asphalt before the stones were placed. There were several instances where the contractor paved over already placed stones resulting in re-application of luminescent stones in those areas. Because of these complications, the south side of the surface does not have stones. A pictorial summary of the process is shown below.

The prepared and leveled sight is shown below in Figure 4-20.

Figure 4-20. Prepped and leveled asphalt site, prior to application.

Asphalt was delivered in multiple batches over the course of two days because of the limited size of the truck. Below in Figure 4-21 on the left is the first batch being unloaded from the truck and

Figure 4-21. Truck used to transport and unload asphalt (left) and smoothing of asphalt by hand after unloading from the truck (right).

on the right the preliminary smoothing prior to rolling with the roller.

After manual smoothing, stones were dispersed by hand in the density mentioned prior and the results after the first rolling are shown below in Figure 4-22. As seen in the right figure, the end of the section was very thin. There were several miscommunications with the contractor about where to stop depositing stones. As a result, many were deposited in these thin layers that the contractors subsequently paved over to increase asphalt thickness, resulting in a smaller portion

of asphalt being covered with stones than anticipated. In Figure 4-23, the last phases of the installation are shown and a glimpse of the stones under the roller where you can see a faint glow is shown.

Figure 4-22. Roller smoothing asphalt with the stones integrated (left) and the asphalt after the first batch was unloaded and smoothed (right).

Figure 4-23. Contractors smoothing the last section of the installation (left) and a glimpse of the embedded stones underneath the smoother (right).

Overall, the stones were well embedded in the asphalt but there were several poorly paved areas where the asphalt is not homogeneous. We attribute this to inferior asphalt equipment and cold-asphalt which was rolled at an un-optimal temperature according to the contractor. These inconsistencies can be seen in both of the zoomed out and zoomed in images seen below in Figure 4-24.

Figure 4-24. Zoomed-out images showing the “cold-rolled” areas that do not look homogeneous (left) and a zoomed-in image of one of these areas (right). In the “cold-rolled” sections the stones were not embedded well (right).

Initial Nighttime Results

Because of the high degree of ambient lighting at TERL, the glowing installations did not stand out as much as we anticipated based on our laboratory scale experiments in a perfectly dark enclosure. Results during the night of the concrete (Figure 4-25) and asphalt (Figure 4-26) installations can be seen below. It proved to be difficult to obtain nice images unless immediately next to the installations which could result in difficulties obtaining high quality time lapse images and relevant luminance data. We aim to work with TERL to try and schedule nights when lighting can be decreased or even turned off. Further, we may have to change the position of our cameras to be placed more immediately on top of the installations than they are. This may require new cameras that are stable outside of the electronic enclosures we designed.

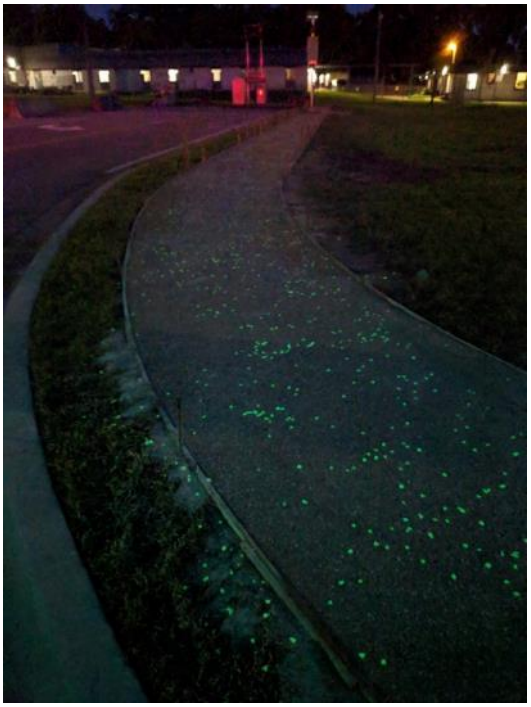

Figure 4-25. Glowing stones on the first night following installation. The surrounding ambient lighting severely hindered observation of the stones' performance.

Figure 4-26. Glowing stones embedded in the asphalt. Like the concrete installation, these proved to be difficult to observe from afar because of the surrounding overhead lighting.

Preliminary Analysis of Stones in Concrete and Stones in Asphalt Installations

Nighttime Results: Time-Lapse – Iteration 1

As detailed in Deliverable 2C, there were 3 Raspberry Pi time lapse cameras initially installed within weatherproof enclosures, one on the concrete and two on the asphalt. They were installed mainly for live updates throughout the day and nighttime. However, with the high degree of surrounding light and exposure settings possible, the quality of these photographs was not up to our expectations during the nighttime. Shown in Figure 4-27 are a series of representative images at noon and 7pm on 10/6/18 for the concrete and asphalt. As seen for both of the nighttime images, the stones are not visible at all. This was a result of having to turn the exposure of the cameras down to block out the surrounding light, but this also resulted in minimal visibility of the stones. It should also be noted that the luminance readings were all drowned out by the surrounding light and there is no noticeable decay.

Nighttime Results: Time-Lapse – Iteration 2

Following the difficulties with the Raspberry cameras, we installed three new time lapse cameras made by Brinno that are specifically suited for nighttime photography. These were installed outside of and on top of the prior electronic enclosures in their own weatherproof casing. Rather than being controlled by a Raspberry Pi, these time lapse cameras cannot be controlled remotely.

Figure 4-27. Raspberry Pi time-lapse photographs on 10/6/2018 at 12 pm (top images) and 7 pm (bottom images). Images on the left are of the concrete installation, and those on the right are of the asphalt.

Photographs are uploaded to an SD card that must be manually uploaded to a computer by TERL staff onsite. Further, batteries need to be replaced intermittently, unlike the equipment (including Raspberry Pi Cameras) contained within the electronic enclosures. An image showing the original electronic enclosure with the Brinno time-lapse camera mounted on top (indicated with "A") is shown in Figure 4-28.

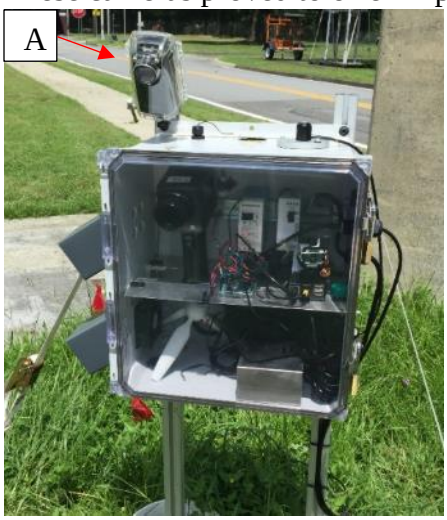

Figure 4-28. Electronic enclosure with Brinno time-lapse camera (A).

These cameras proved to offer improvement over the Raspberry Pi cameras. Shown in Figure 4-29 and Figure 4-30 are images at 7 pm (near dusk) and 8:30 pm for the concrete installation on 10/6/18. Immediately apparent is the difference between these and the Raspberry Pi photographs at 7pm where it appeared to be very dark – this is related to the exposure setting which was decreased to limit the surrounding light. At 8:30 pm where it is sufficiently dark and the stones are glowing strongly, it is still difficult to see them however except for the shaded portion on the far left side of the image in the shaded region. Images appear slightly better for the asphalt installation where the oak tree overhead provides more obstruction from the surrounding light sources; images at 7 pm (near dusk) and 8:30 pm on 10/6/18 are shown in Figure 4-31 and Figure 4-32. While these images are an improvement over the Raspberry Pi cameras, this has still not remedied the difficulties associated with measuring luminance with the meters contained within the electronic enclosures. We have attempted to extract the pixel intensity over time from the Brinno images to track the decay in intensity, but this has proved difficult because of the surrounding light sources.

Figure 4-29. Brinno time-lapse photograph of the concrete installation at 7 pm on 10/6/2018.

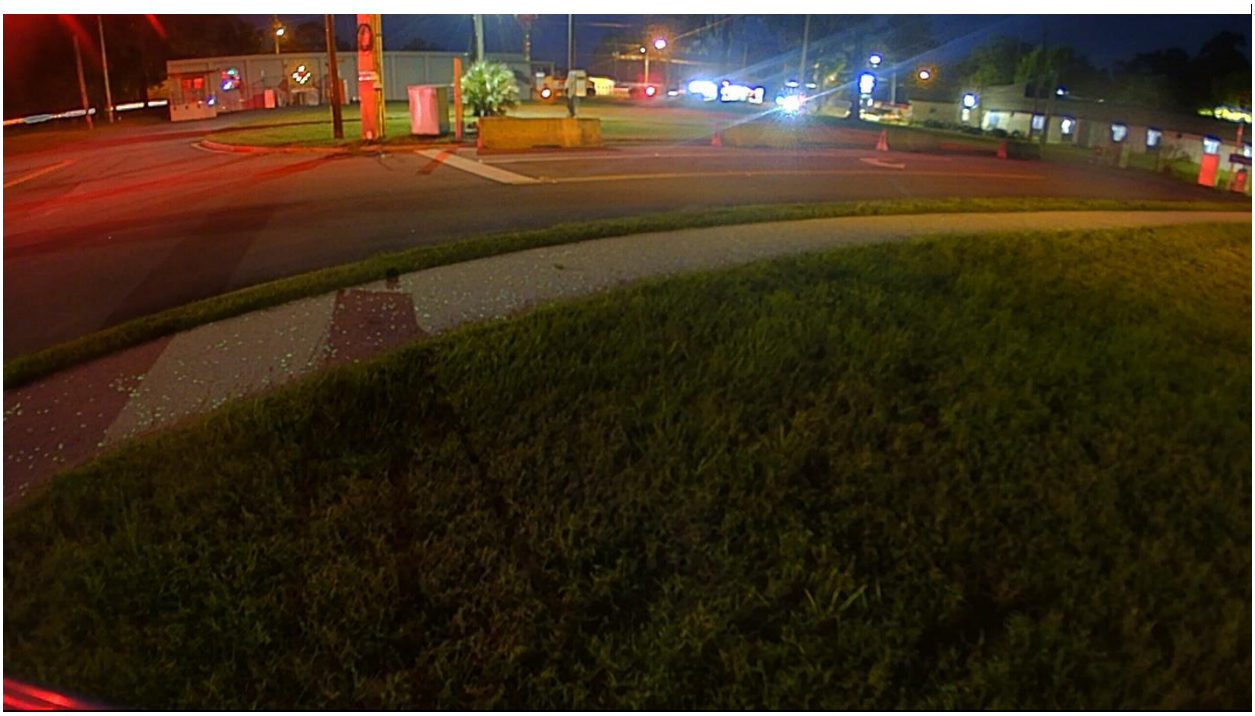

Figure 4-30. Brinno time-lapse photograph of the concrete installation at 8:30 pm on 10/6/2018.

Figure 4-31. Brinno time-lapse photographs of the asphalt installation at 7:00 pm on 10/6/2018.

Figure 4-32. Brinno time-lapse photographs of the asphalt installation at 8:30 pm on 10/6/2018.

Nighttime Results: Time-Lapse – Iteration 3

The prior difficulties with image and luminance measurements made it clear that we need to remove all or most surrounding lighting at TERL. Our initial proposition was to turn off as many overhead lights on select, predetermined nights, but this was not possible because of security concerns. We then turned to the idea of an enclosure that could easily be removed and placed over a predetermined area of stones. The final concept we decided on was a 2ft x 2ft x 2ft enclosure constructed out of 80/20 struts that would afford mounting options inside and outside. Further, the enclosure was outfitted with a moveable aperture made of PVC piping that would allow the luminance meter to see into the enclosure; it was lengthened in order to limit the amount of surrounding light that would ultimately make it into the enclosure. A Solidworks drawing of the enclosure and a photograph onsite is shown in Figure 4-33. As seen, the aperture is mounted to a vertical strut that allows it to be moved up and down on demand. Its angular position with respect to the horizontal is also flexible. There is a curtain secured with pins on the aperture side of the enclosure in order to adapt to the aperture position. Mounted inside the enclosure is another Brinno time lapse camera.

The dark enclosure box is placed over the same, pre-marked area of concrete at a varying but prescribed time each day such that the sun's angle of incidence, θ, is kept constant to ensure constant solar exposure. The angle of incidence was calculated according to the following:

$$\cos\theta = \sin\delta\sin\phi\cos\beta - \sin\delta\cos\phi\sin\beta\cos\gamma + \cos\delta\cos\phi\cos\beta\cos\omega + \cos\delta\sin\phi\sin\beta\cos\gamma\cos\omega + \cos\delta\sin\beta\sin\gamma\sin\omega$$

where δ is the declination angle, ϕ is the latitude, β is the slope angle, γ is the surface azimuth angle, and ω is the hour angle. β and γ are assumed to have a value of 0°. The latitude of Tallahassee is 30.4383°N. The angle of incidence was calculated for the first day the dark enclosure was placed at 5:30 pm on 10/25/18. The hour angle and local time of day for all subsequent days was determined such that θ remained constant. A schedule was created for

Figure 4-33. Left) Solidworks model of dark box enclosure. The only additional components to this model not shown are the blackout curtains covering the front opening that go around the PVC aperture and the time-lapse camera, which is mounted on the inside of the box looking straight down at the concrete. Right) Experimental setup at TERL facility in Tallahassee. The inner diameter of the PVC pipe is 2 inches. With a 1° acceptance angle for the luminance meter, the box can be up to 9.5 ft away and still look entirely through the PVC tube to the stones.

FDOT to ensure that the enclosure is placed at the appropriate time each day; an excerpt is shown in Figure 4-34. This allows us to know if the box was placed which is important for data analysis.

The time lapse camera inside the dark enclosure was programmed to take a picture every minute.

Month	Day	Year	Place Box Hour	Place Box Minute	Sun Angle	Sunrise Hour	Sunrise Minute	Sunset Hour	Sunset Minute	Dark Box Placed? Y/N	Time Placed?	Time Removed?
10	25	2018	17	30	73.96	7	53	18	50	Y	17:30	N/A
10	26	2018	17	29	73.91	7	53	18	49	Y	17:28	8:35
10	27	2018	17	28	73.92	7	54	18	48	Y	17:30	8:25
10	28	2018	17	26	73.93	7	55	18	47	N	N/A	8:30
10	29	2018	17	25	73.94	7	56	18	46	Y	17:26	N/A
10	30	2018	17	24	73.94	7	56	18	45	N	N/A	8:36
10	31	2018	17	23	73.91	7	57	18	44	Y	17:23	N/A
11	1	2018	17	22	73.92	7	58	18	44			
11	2	2018	17	21	73.92	7	59	18	43			
11	3	2018	17	20	73.92	7	59	18	42			

Figure 4-34. Example of schedule followed by FDOT staff for placement of the dark box enclosure.

The photos are stitched together and saved as a .AVI video file and analyzed in MATLAB. Pyranometer data is continually recorded throughout the day and saved to a .csv file which is then analyzed in MATLAB. The pyranometer data is discussed in more detail later in the report. The luminance data is also saved to a .csv file.

Data Analysis

The files from the time lapse camera are saved as .AVI video files where each frame of the video is a photo taken at 1-minute intervals. A MATLAB code was written that analyzes the average and maximum pixel intensity for each individual stone as well as the conglomerate of stones within the selected area. An exemplary photograph is shown in Figure 4-35; the red box indicates the area where pixel intensity

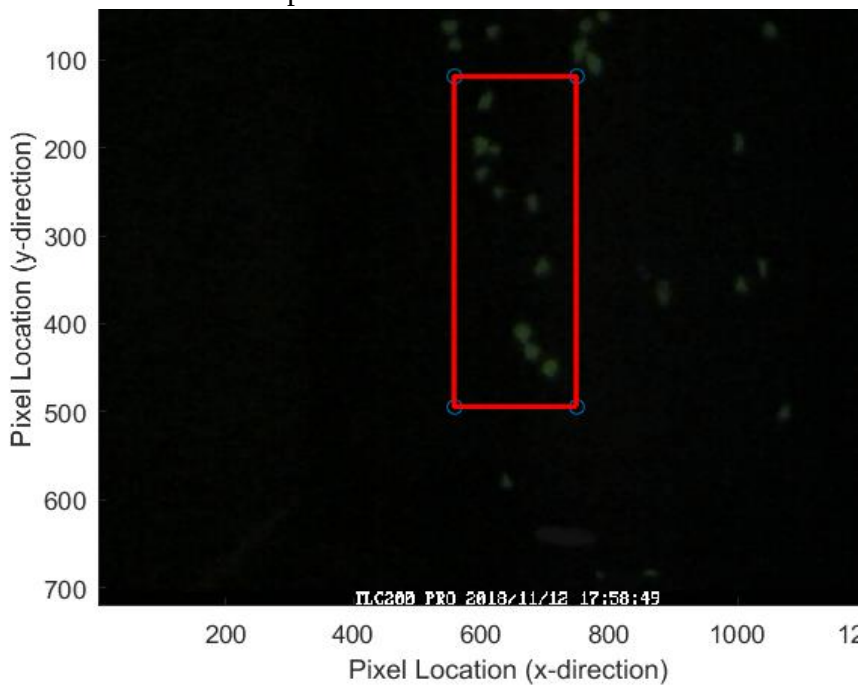

Figure 4-35. Single frame from AVI video file. The user selects the area of the image to be analyzed, indicated in red. All subsequent frames are then cropped to this selected area.

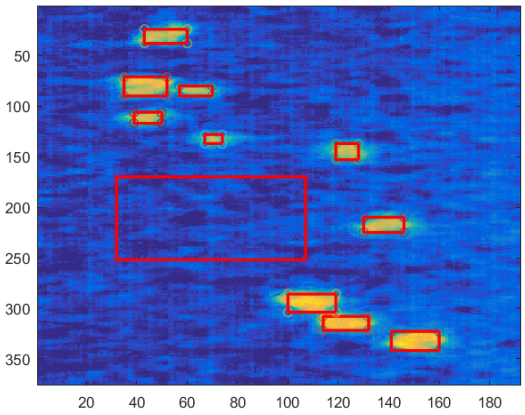

Figure 4-36. Boundaries for all stones as well as an area containing no stones that serves as the baseline intensity.

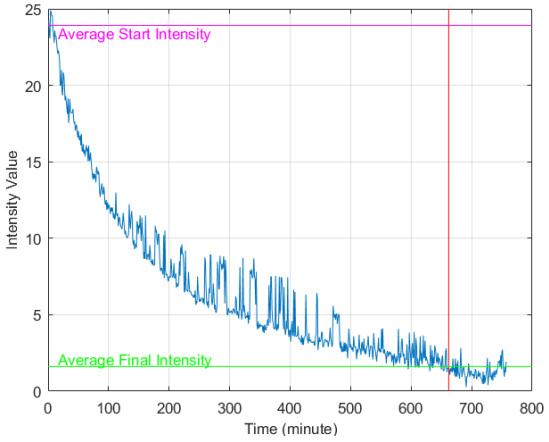

Figure 4-37. Averaged pixel intensity from Figure 4-34.

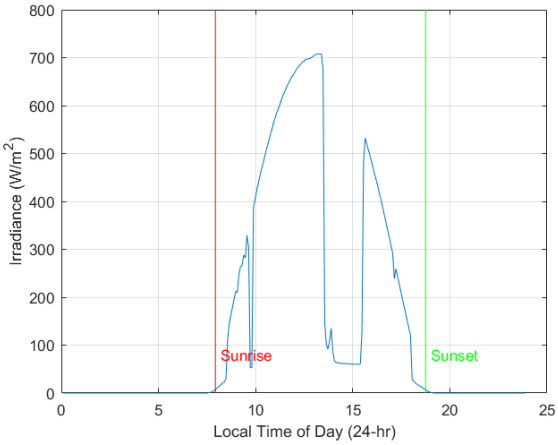

Figure 4-38. Pyranometer data captured from October 30th, 2018. It should be noted that there is a sharp decrease at around 1:30 pm and continues to around 3:30 pm due to cloud coverage.

data is extracted from. The user then defines boundaries around each individual stone and an area without any stones that serves as a baseline subtraction, as indicated in Figure 4-36. The MATLAB code iterates through each frame of the video throughout the night and collects data from the selected areas. The overall average of all red boxed areas, after the baseline intensity values have been subtracted is shown in Figure 4-37 in blue. As seen, there is a characteristic exponential type decay that is expected for these stones. The average final intensity (green line) is the average of the final 20 intensity values. The average starting intensity (magenta line) is the average of the first 10 intensity values. The decay time is calculated as the time it takes for a moving average of 30 points to be equal to or less than the final intensity. As seen, for this day the decay time was greater than 650 minutes, or about 11 hours.

The pyranometer is mounted horizontally on top of the equipment box and records data during the day, every day. The stones take less than 8 min to reach maximum charge, and therefore, when analyzing how weather affects the stone intensity, only the final 15 minutes prior to sunset are be considered. Shown below in Figure 4-38 are pyranometer data from a relatively sunny day except for cloud cover from around 1:30 pm to 3:30 pm.

With an established method for gathering and interpreting the time-lapse video data and pyranometer data, these can be further coupled to give a better representation of the behavior of the decay times at different solar radiation levels. As more data points are added, comparisons can be made in the trends between different times before sunset as well. Results showing the decay time verses the radiation received for the 15 minutes prior to placement of the enclosure are shown in Figure 4-39. Depending on the cloud coverage

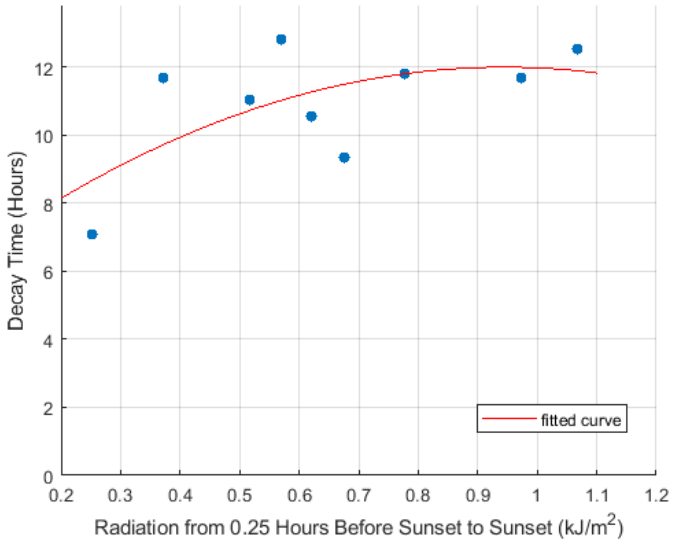

Figure 4-39. Decay time (hours) plotted against the amount of radiation received (kJ/m^2) by the stones 15 minutes prior to sunset for the average pixel intensity.

during the final 15 minutes of the day, intensity decay time varied from around 6 hours to 12 hours proving that these stones have the ability to last throughout the night. However, the intensity of the glow as perceived by the human eye should be further explored. This will have to be accomplished by translating these pixel intensity values to luminance and/or interpretation of the luminance measurements. However, there are still difficulties regarding the luminance measurements that are related to a combination of factors. The first is the attenuation of light through the electronic enclosure which appears to have become more opaque with time. The second and likely more pertinent barrier is the precise placement of the aperture each day which is required because of the very small acceptance angle of the luminance meter. We have considered options such as mounting the luminance meter within the electronic enclosure like the camera, but it is not weatherproof, not battery powered and must be connected to a PC continuously to upload the data. The later can be accomplished fairly easily but we are worried about exposure to the weather if it is kept outside of the electronic enclosure. Thus we anticipate that we will not be able to deliver consistent and reliable luminance data other than through translation of the pixel intensity of the images acquired via time-lapse photography.

Over the next 6 months the plan is to focus primarily on acquiring more data points to populate Figure 4-39. As seen, there are only a handful of data points currently because this was not constructed until 10/25/18. There were several days where data was not capable of being acquired, either due to weekends or unavailability of personnel to place the enclosure at the appropriate time of day. We hope to be able to accurately correlate the amount of solar radiation, as well as other weather behavior such as rain and overall de-activation of stones to the expected decay times.

Assessment of Particle Raveling and Continued Data Analysis at TERL

Particle Attrition and Raveling after ~1 year

On April 23rd 2019, about 1 year after installation, the UF team took a series of images of the concrete and asphalt pathways to try and assess the degree of particle attrition and raveling. Overall, our conclusion is that both pathways remained relatively unchanged. We could not observe any attrition or raveling on the concrete walkway.

Asphalt Pathway

Below in Figure 4-40 is a photograph from a time-lapse camera installed at the asphalt pathway taken on June 15th, near the date of construction. As seen, the stones are well distributed. Select photographs from later dates using the same time lapse camera (12/22/2018, 2/21/2019 and 4/03/2019) are shown in the following images in Figure 4-41 Overall, the images show no grossly apparent changes in the stone density. However, it is difficult to assess how well the stones are integrated into the pathway and the overall integrity of the installation because the images are taken from within a weather-proof enclosure at a distance fairly far from the pathway.

Figure 4-40. Image taken on June 15th, 2019from within the weatherproof enclosure installed at the asphalt pathway.

Figure 4-41. Images taken from within the weatherproof enclosure installed at the asphalt pathway on 12/22/2018, 2/21/2019, and 4/03/2019.

A representative zoomed out, top-down, perspective of the asphalt alongside a zoomed in portion is shown below in Figure 4-42. Again, the stones are relatively well distributed. The inhomogeneity that does exist results from the fact that particles were sprinkled by hand in pre-designated area to ensure consistent average density in each 4 ft. length. The zoomed in image on the right (representative area is indicated by the yellow border in the left image) gives a better representation of how well the particles are bound to the asphalt.

Figure 4-42. Top-down view of the asphalt installation (left). Zoomed-in image showing the integration of the stones in the asphalt (right).

Figure 4-43 shows a horizontal perspective of the stones integrated into the asphalt in order to ensure the stones are level with the asphalt surface. Several locations were photographed and there were no noticeable areas where the stones did not appear to be flush with the surface of the asphalt.

Overall, our conclusion is that the asphalt pathway remained unchanged over the course of approximately 1 year, with the exception of areas where the asphalt was cold rolled. It should be noted however that these sections were well in the minority compared to the other areas and should not be expected for a higher quality asphalt installation. We attribute this solely due to the contractor's methodology rather than any inherent difficulties integrating the stones well into the asphalt surface.

Figure 4-43. Horizontal image showing that the stone surface is level with surface of the asphalt.

Concrete Walkway

An overview of the concrete installation is shown below in Figure 4-44. The concrete installation is approximately 150 ft. long and extends to the far southwest side of TERL. Overall the concrete walkway is in good shape after one year and there is no noticeable deterioration, attrition or raveling of the glowing stones. The only noticeable defects are superficial in nature, related to where grass or weeds have grown in around the edges or between the saw cuts. At this zoomed out scale the stones are not noticeable like the smaller stones in the asphalt. This is because the contrast between the stones and concrete is poor.

To see the stones more clearly, zoomed in images are shown in Figure 4-45. On the left is a representative top down view of the concrete, and the right an even more zoomed in top down view with only a few stones in view. The glowing stones can be distinguished from the other pebble aggregates in the concrete by their size; the stones are typically much larger. We could not find evidence of either cracking or loosening of the stones from the surrounding concrete. The only noticeable change is that the color appears to be less green than when they were originally installed. However, we have yet to conclusively assess the impact of this, if any, on the luminance. Our preliminary analysis does not show any decrease in performance, at least within

the limits that were are capable of assessing. Overall, our conclusion is that the stones remain well integrated in the concrete.

Figure 4-44. Zoomed-out images of the concrete walkway. At this scale, the stones are not easily discernable. Weeds have grown in along the edges of the concrete and within the saw cuts, but there is no noticeable deterioration of the installation.

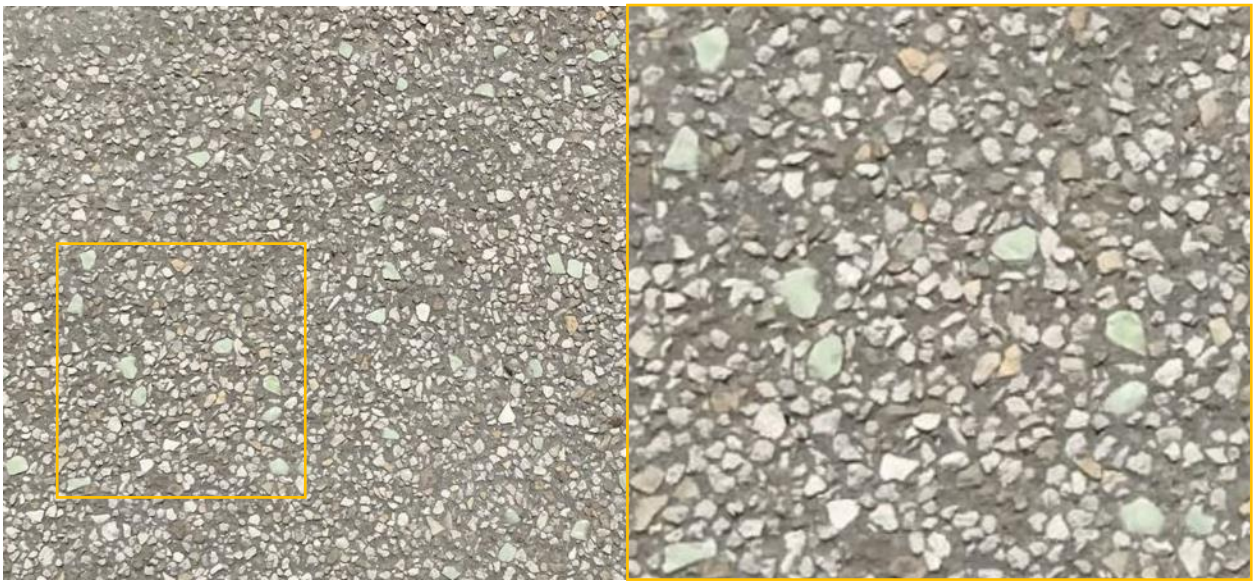

Figure 4-45. Top-down view and zoomed-in images of the concrete. Glowing stones can be recognized by their larger size, compared to the other exposed aggregate particles. Although only a single area is shown, this is representative of the entire installation. No attrition or raveling is observed, but the color of the stones has noticeably faded.

Concrete Pixel Intensity

Pixel intensity was recorded from the dates 10/19/2018 until 3/8/2019 using the dark enclosure coupled with time-lapse camera described in prior. Overall, maximum pixel intensity recorded by the camera and the pixel intensity recorded 8 hours after sunset show a decline over the dates observed. Results are shown below in Figure 4-46 as orange (maximum) and blue (8 hours after sunset) circles overlaid with linear trend lines for visual purposes. Results are limited to these

dates and this installation only because the enclosure could not be placed at appropriate times by TERL staff as the sun began to set later and later in the evening, well after 5pm when most TERL staff were not available to move the dark enclosure. Nevertheless, results show a clear downward trend that should be investigated further under more appropriate and controlled conditions.

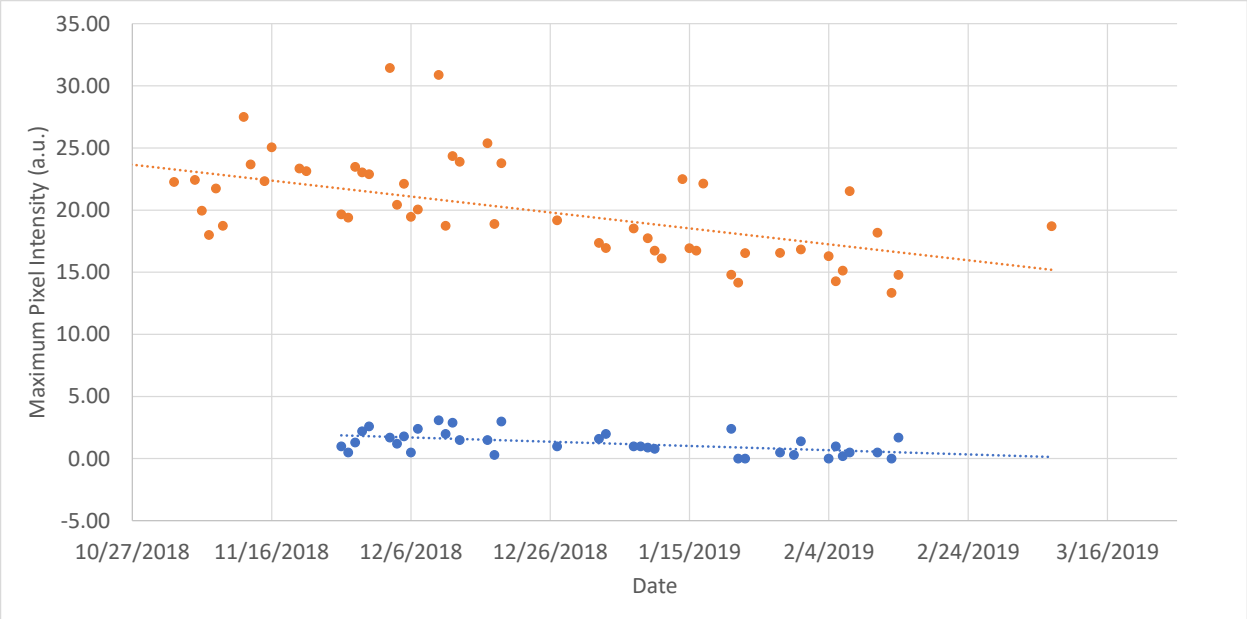

Figure 4-46. Maximum pixel intensity and pixel intensity recorded 8 hours after sunset for the stones on the concrete walkway. Orange dots represent maximum pixel intensity and blue the intensity, after 8 hours. Lines are linear trend lines for visual purposes only.

Chapter 5 **University of Florida Concrete Installation**

Installation

In an effort to reduce the ambient lighting and ease access to data acquisition equipment, a 30 foot by 8 foot sidewalk with photoluminescent stones was installed at the University of Florida campus between the dates of 5/6/2019 and 6/23/2019. Every effort was made to install the stones in an area with limited lighting but one that is also frequented by foot traffic in order to increase visibility. A second, very small scale installation was also installed at UF's energy park away from any ambient lighting in order to acquire even higher fidelity data with nearly zero artificial lighting.

A summary of the installation and results is provided here. A highly trafficked sidewalk on campus between the Mechanical and Aerospace Engineering A Building and New Physics Building was selected because it proved to have low ambient light levels compared to most locations and approval by the University was straightforward because the sidewalk section is not a designated ADA sidewalk. The contractor performing the installation was North Florida Concrete Coatings and Countertops, whom we worked with prior on the installation at TERL.

Figure 5-1. Glowing UF logo fabricated by placing Emerald Yellow glow stones on double-sided carpet tape.

Two of the major goals of this installation were to ensure a very high stone density, as well as include logo-type designs made of the stones. Because the installation was to be performed at the University of Florida, we decided on UF themed designs. Based on our prior experience at TERL when placing stones, we decided to try a new approach using pre-fabricated sheets rather than placing the stones individually by hand in the wet concrete. The reason for the pre-fabricated sheets was rooted by two different motivations. First, these pre-fabricated sheets would ensure only a single layer of stones are used because we could dictate their positions precisely. At TERL, stones were dropped into wet concrete and the exact position was uncertain, meaning that an excess of stones would have to be used if a single layer of stones is desired on the surface. Because of their cost (~$50/lb) we thought that it would be strategic to limit the amount needed. The second motivation for prefabricating shapes was because of the expected time required to place stones in very high density, in precise shapes, and we were worried about the concrete curing before we had time to place everything appropriately. We decided to use carpet tape because of its strong adhesion properties and because it is porous, an important property to ensure adhesion to the concrete according to the contractor. The plan was to rotate between these

Figure 5-2. Sidewalk after removal of prior (left) and sidewalk after pouring concrete (right).

Figure 5-3. The pre-fabricated logos were placed under the concrete by the contractor. Solid sections of carpet tape were flipped, and the bottom, white side is shown. These sections were smoothed but not covered by concrete.

logos, solid sections without logos and inverted logos over the length of the sidewalk. An exemplary pre-fabricated design of one section is shown in Figure 5-1.

Initially on 5/5/2019 the existing sidewalk was removed in anticipation of installation the next day. Photographs after removal and after pouring of concrete are shown below in Figure 5-2. During installation the contractor determined that the large prefabricated sections were not being well integrated into the concrete. Therefore, a decision was made to flip solid sections upside down in order to ensure better adhesion of the stones with the concrete. In Figure 5-3 the contractor can be seen embedding one of the logos under the concrete and smoothing with a trowel, with alternating white sections where the carpet tape was flipped. These white sections were smoothed with the lumber to ensure good adhesion to the concrete.

More than an hour had passed between the time the concrete was poured and when the contractor began embedding the sections in the concrete. This was because immediately following the pour, the cement truck (which

was rented for an hour) poured the remaining concrete at a different, smaller scale installation at UF's Energy Park slightly off campus where we hoped to take time lapse photos without any surrounding lighting (results discussed later). Because of the long time that elapsed, the concrete was already beginning to cure by the time the contractor began embedding the prefabricated sheets and it was difficult to make these perfectly smooth. Because these sections were not perfectly leveled, the contractor recommended using a polisher to smooth, level and expose the

Figure 5-4.One week later, the tape backing was removed, and the stones were mostly well integrated but there were sections that did not adhere well to the concrete because it cured for too long (left). Contractor using polishing machine to smooth elevated and uneven sections (right).

stones in those sections. Therefore, we left the installation to fully cure for 1 week and returned the following week to remove the carpet tape backing and polish. Figure 5-4 on the left shows the carpet tape backing being removed and on the right the contractor polishing the concrete, especially the logo areas that were not perfectly level. The areas underneath the carpet tape backing proved to be well integrated in some sections and not as well in others because the concrete was too cured to make it into some of the small spaces between stones and ensure good adhesion. A reflection of this can be seen in Figure 5-8 towards the end of this report where there are some sections glowing well and others with only concrete that were patched over.

Unfortunately, sections of concrete with the logos embedded did not respond well to the polisher. Stray tape beneath the concrete was caught in the device in several areas and ripped up large sections of the installation. These sections were not salvageable and we ultimately made a decision to rip these sections out and start over in a little more than a month (6/23/2019) when

the contractor could fit us into his schedule. An exemplary image of the exposed tape that was caught in the polishing device is shown in Figure 5-5 on the left and the removed sections filled in with freshly poured concrete are shown in Figure 5-5 on the right.

On the new portions we instead used a stencil type method to make “UF” logos in the concrete rather than attempt the pre-fabricated method again. A series of images showing the installation

Figure 5-5. Representative image of the tape that was caught in the polishing machine (left) and freshly poured concrete in the sections with logos that were removed (right).

process is shown below in Figure 5-6. The image on the left is the University of Florida logo where the stones are being placed by an undergraduate student. The contractor in the next image then used a trowel to embed the stones in the concrete. After washing away the top surface, the logo was revealed, as shown on the left image of Figure 5-7. In Figure 5-7 on the right, the entire installation is shown. It is composed of alternating panels of “UF” logos and sections with high density sections.

Figure 5-6. Stencil used to create the UF logo out of glowing stones (left). Contractor using a trowel to embed the stones in the concrete (right).

Figure 5-7. Left) Zoomed-in imaged of the logo after removing the top layer of concrete. Right) Image of the entire installation showing alternating logos and high density stones.

Time-Lapse Photography

Time lapse images of the installation have been acquired throughout the nighttime. A snapshot of the installation soon after sunset (not edited) is shown in Figure 5-8. For anyone at FDOT who would like to see time lapse videos of the installation during the entire nighttime (sent to Ron Chin and Matt Dewitt prior), both zoomed on a logo and of the entire installation, please email me at jscheffe@ufl.edu and I will provide electronic credentials. Following this are a series of three time-lapse images of the installation near peak intensity after sunset, midnight and 3 am, respectively.

Figure 5-8. Snapshot from camera after sunset.

Figure 5-9. Photograph of the installation near peak intensity after sunset.

Figure 5-10. Photograph of the installation at midnight.

Figure 5-11. Photograph of the installation at 3 am.

Concrete Installation at the University of Florida's Energy Park

In an effort to acquire more quantitate data, a second installation with randomly distributed stones was fabricated at UF's Energy Park where we have control over local lighting and keep it off during most evenings. Here we have a permanent time lapse camera installed directly overhead the installation and the same electronic enclosure that was installed at TERL with a pyronometer installed in order to acquire total horizontal solar irradiation. An image of the installation with the time-lapse camera installed directly overhead is shown in Figure 5-12.

Data Analysis: Methodology

The pyranometer is set up approximately three feet from the concrete stone installation. It collects a reading for the irradiance of the sun every 300 seconds. This data is logged automatically into an excel file which contains all the irradiance measurements for one day from 12:01 am to 11:54 pm.

Once the pyranometer data is collected for one day, it is processed with a Matlab code that calculates the total irradiance for the entire day and the total irradiance for the last 15 minutes of the day. These values represent the summation of irradiance measurements for the whole day and the last 15 minutes before sunset. Using the total irradiance measurements for the last 15 minutes before sunset, the pyranometer data is then classified into three categories: a sunny day (Irradiance > 0.3 kJ m^{-2}), a moderate day (0.15 kJ m^{-2} < Irradiance < 0.3 kJ m^{-2}), and a cloudy day (Irradiance > 0.15 kJ m^{-2}). These values were determined based on the distribution of pyranometer data collected during the summer of 2019. The classification of these measurements is used to classify and analyze the Time-lapse Video data that is collected from the concrete stone installation.

After the photoluminescent stones were installed in the UF Energy Park, a time-lapse camera was set up above the installation. The camera takes pictures of the stones in one-minute intervals throughout the night. By running the photos of this decay process through a custom Matlab code, the intensity of light can then be classified through an arbitrary measurement of pixel intensity.

An excel spreadsheet was created which contained the time of sunset for every day of the year. Once the video was taken for a certain date, the video was manually scanned for the sunset time, then the exact video frame at which sunset occurred could be calculated.

The Matlab code which was used to analyze the time-lapse data is a modified version of a previous code used to calculate the decay time for the stones, discussed in Deliverable 2D. The code takes the photo data of each frame, starting at sunset, and translates it into a temperature map. This means that the stones which produce light at night are classified as high temperature readings and the concrete surrounding the stones is classified as a low temperature reading. This enables the code to then analyze the pixel intensity of the stones as though it were a temperature differential between the concrete and the stones, accounting any differences in color. This allows an arbitrary intensity value to be assigned to each pixel of each time-lapse photo.

Once the temperature map has been created, the starting frame is cropped, and ten stones are selected for each day (kept constant during each daily analysis). A baseline of concrete is also selected. The code goes through each of the eleven previously selected areas of each video frame (one for each of the ten stones and one for the baseline) for an eight hour period after sunset. This code then collects information about the average pixel intensity in each area and the maximum pixel intensity in each area. Afterwards, the values for the baseline area are subtracted

Figure 5-12. Time-lapse camera and concrete installation with Emerald Yellow glow stones embedded at UF's Energy Park.

from the stone measurements. This normalizes the data and accounts for any light pollution in the surrounding area. Then, the measurement for all ten stones is analyzed to calculate the maximum average pixel intensity for each frame and the absolute maximum pixel intensity for each frame. The maximum average pixel intensity is integrated across 480 frames (8 hours) to collect a value for the Integrated Pixel Intensity. The maximum value of the maximum pixel intensity is then recorded as the Peak Pixel Intensity value. In a separate Matlab text, the aforementioned process is repeated but, rather than finding the values at each frame after sunset for eight hours, the code selects frames that occur one hour, two hours, three hours, and eight hours after sunset. The maximum average pixel intensity is then calculated for these frames to illustrate the decay of the stones over time.

Data Analysis: Results

Representative time lapse images from 6/11/19 immediately following sunset, after midnight and just before sunset are shown below in Figure 5-13. As seen, the stones continue to glow for the duration of the night, but do have noticeable decay. High resolution videos with data shown every minute can be obtained on request from FDOT via email at jscheffe@ufl.edu. Pixel intensity from the images below is shown in Figure 5-14, where each frame is representative of one minute. As seen, after about 450 minutes (> 8 hours) the pixel intensity decreases by about a factor of 3 from about 150 to 50. In reality, the decrease is substantially greater but the initial peak intensities of the stones are not captured using this methodology because the surroundings do not shift from light to dark instantaneously like they do in laboratory settings. Thus, when the stones are most intense, before it is completely dark, we are not measuring their performance. Please see prior

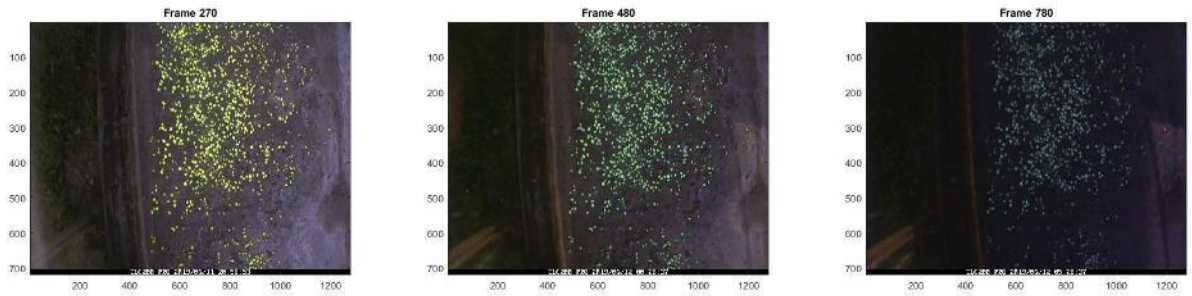

Figure 5-13. Images taken at 8:58 pm (left), 12:28 am (center) and 5:28 am (right).

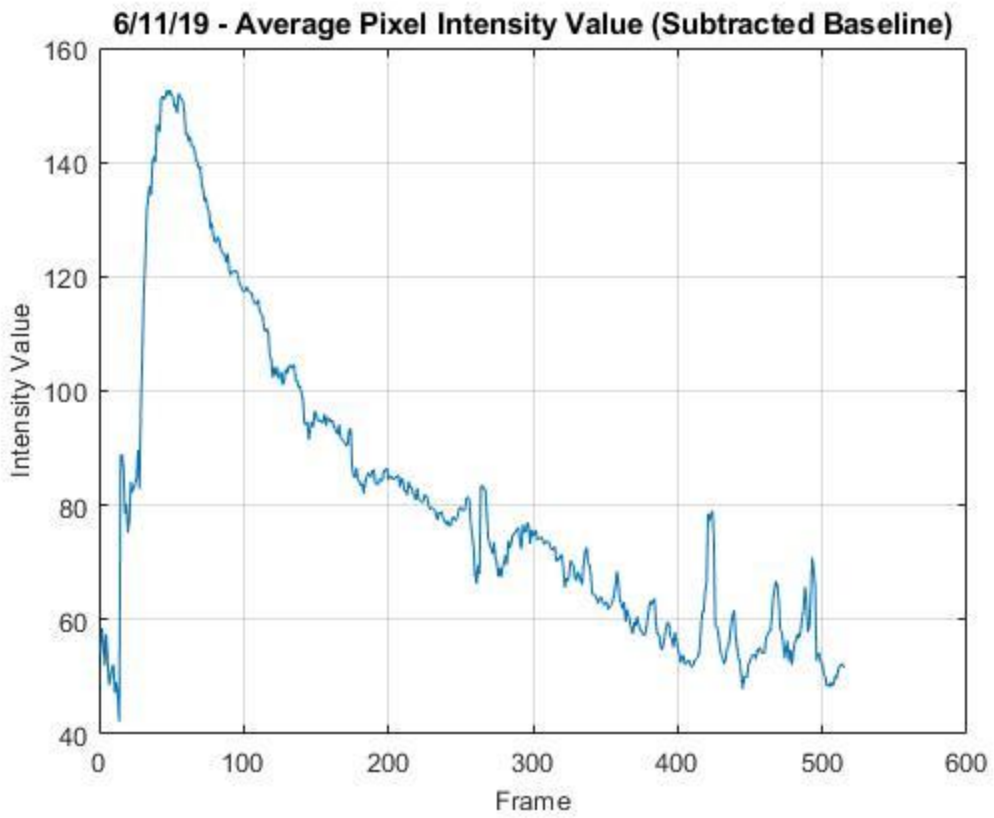

Figure 5-14. Pixel intensity shown vs. Frame (1 frame = 1 minute) for the images shown in Figure 5-13.

"Afterglow Behavior" section for expected decrease in intensity verses time in laboratory settings.

Interestingly, the amount of sunlight prior to nighttime does not have an observable effect on the performance of the stones. We have grouped data according to sunny, moderate and cloudy days as described in the methodology section and representative pyranometer data for these days is shown in Figure 5-15. The maximum pixel intensity and pixel intensity 8 hours after sunset recorded for all dates where data has been analyzed is shown below in Figure 5-16. In both cases

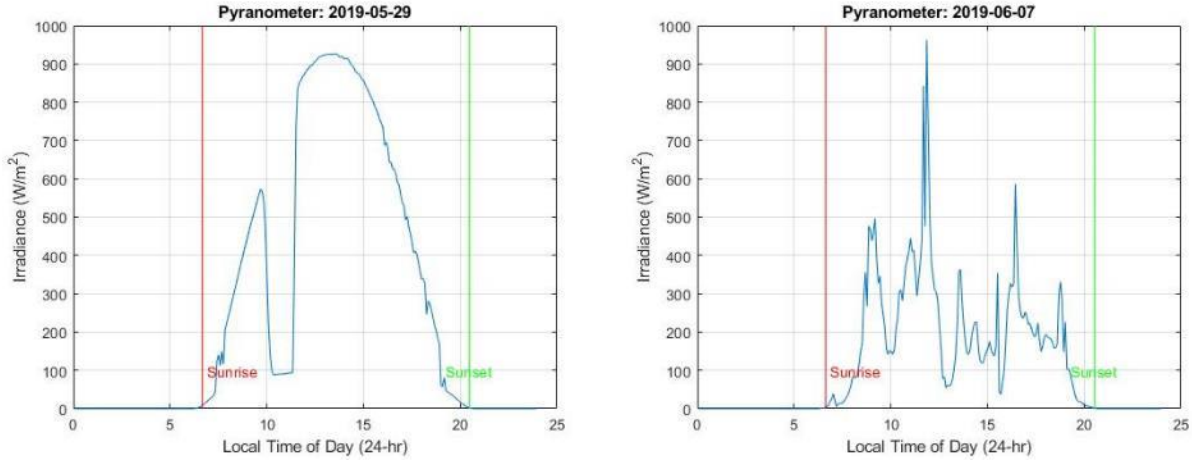

Figure 5-15. Solar irradiance on a sunny day (left) and cloudy day (right).

the data appears scattered and there is no obvious difference between sunny, moderate or cloudy days. In the next section we attempt to replicate these results in the laboratory to confirm that after the initial intensity, which does increase with increasing irradiation, the results tend to converge with time. Also of note is that there is no obvious decay over time, unlike the results form TERL (Figure 4-39) that showed a decrease in intensity over several months. There

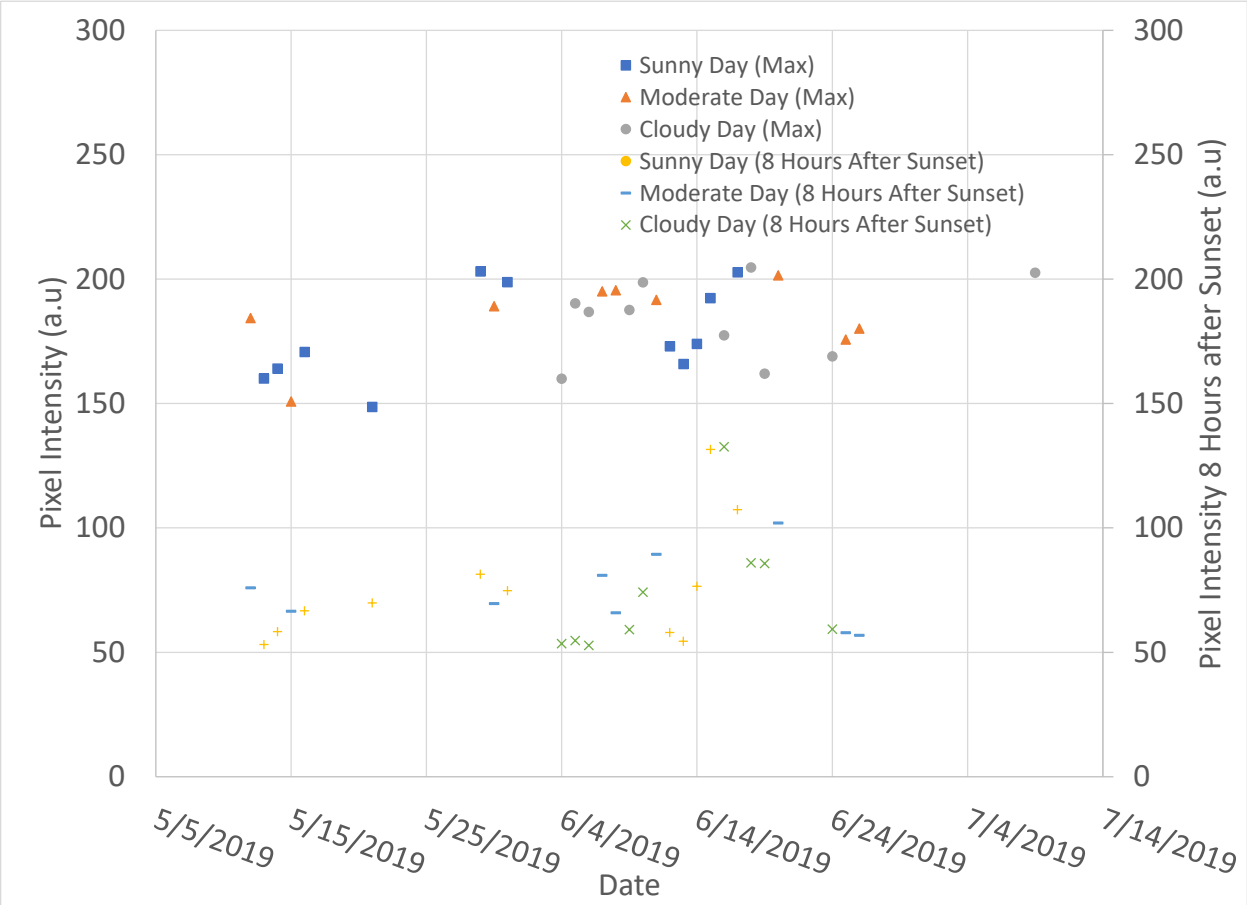

Figure 5-16. Pixel intensity as measured by the time-lapse camera, divided by sunny, moderately sunny and cloudy days. On the left axis is the maximum pixel intensity recorded, and on the right, the intensity measured 8 hours after sunset.

however, there is more uncertainty in the TERL data analysis because of the dark enclosure that was used and flipped at different times each day.

Laboratory Investigation of Incident Radiative Power on Afterglow Behavior

The objective of this section was to characterize the luminance decay of luminescent materials with varying exposure to light with a focus on the emerald yellow luminescent stones that were installed at TERL and The University of Florida. From field data as discussed in the prior section, it was suggested that the varying amount of sunlight didn't have a major impact on the luminance. Thus, the motivation for this project was to reproduce the field-testing conditions and gather data to analyze it.

In order to test this, a power source was set up with two different power outputs. "half power" which correlates to approximately 56 mW and "full power" which correlates to approximately

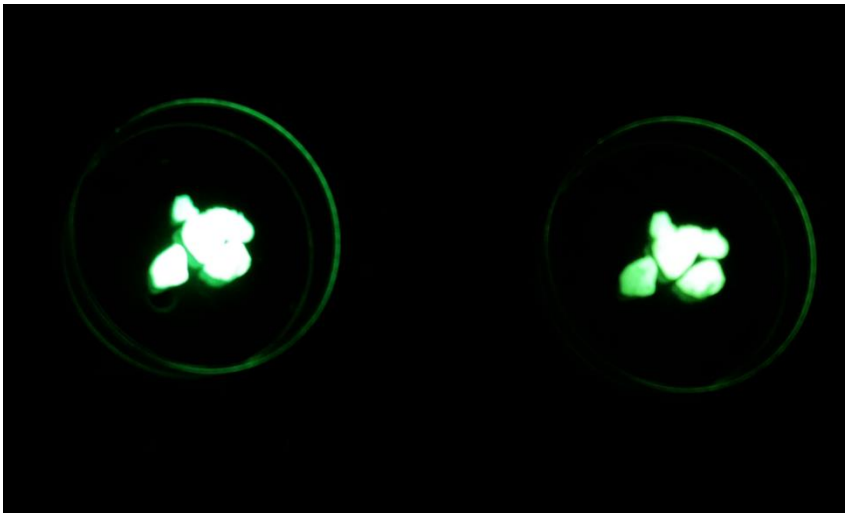

Figure 5-17. Image of the stones immediately after the LED light was shut off at full power (left) and half power (right).

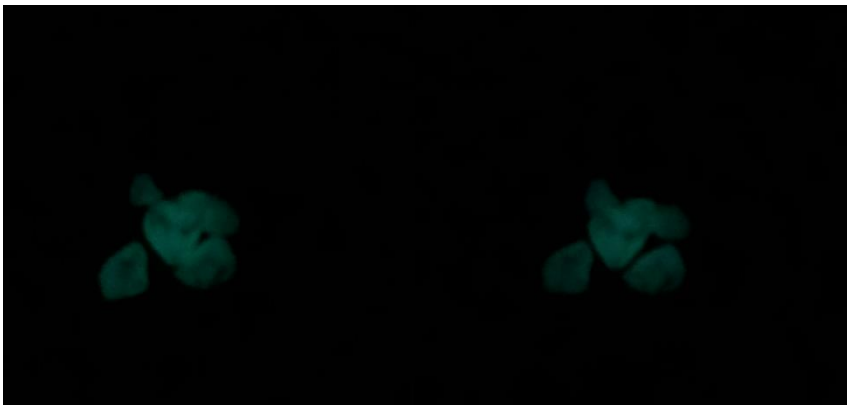

Figure 5-18. Image of the stones 210 seconds into the discharge phase of the stones charged at full power (left) and half power (right).

117 mW. The peak luminance of both cases was 14.99 cd/m^2 at full power and 6.85 cd/m^2 at half power. Both stones exhibited an exponential decay in luminance. Differences in stone performance were observable up until approximately 3 minutes, in which a percent difference greater than 10% was measured. From this, it was concluded that the difference in the amount of sunlight the stones would receive only has a major impact in the first few minutes of luminescent discharge.

Experimental Procedure

The luminescent stone samples were obtained from Ambient Glow Technologies (AGT). Four luminescent stones were placed in a petri dish and placed in an enclosure in which no outside light may touch the stones.

The stones were illuminated, or "charged", by using a white LED light. The stones were charged under the LED light at a power of 117 mW (full power) and a power of 56 mW (half power) for 20 minutes. A luminance meter (Konica Minolta CS-S20) was used to characterize the luminance decay of the sample after the LED light was turned off for both cases. Data points of luminance vs time were taken every 3 seconds for 4700 data points. Additionally, the photos of the stones were captured during the charge and discharge phase of the luminescent stones using a camera controlled by a Raspberry Pi. Images were taken at 15 second intervals, and exemplary images immediately after exposure to the LED and 210s after are shown below in Figure 5-17 and Figure 5-18.

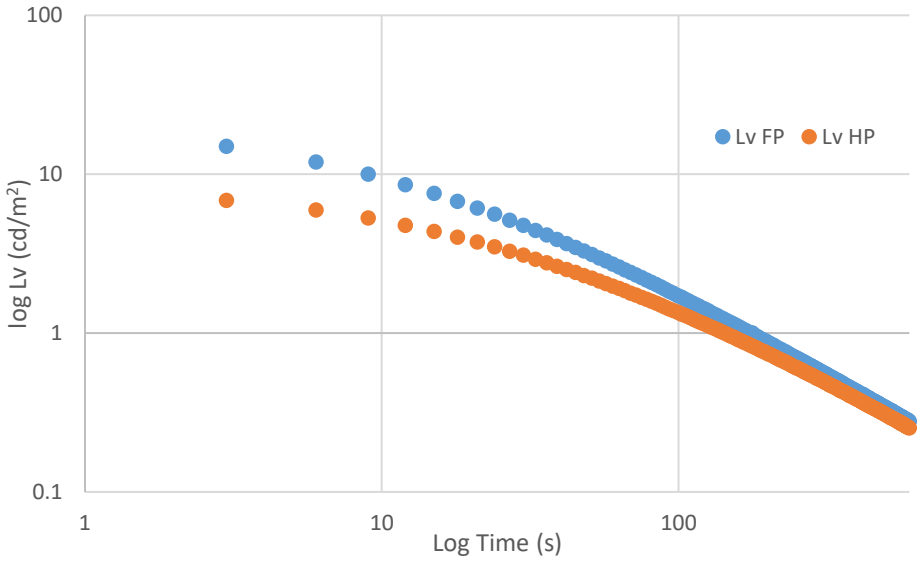

Figure 5-19. Log(L_v) vs. log(t) for the first 10 minutes.

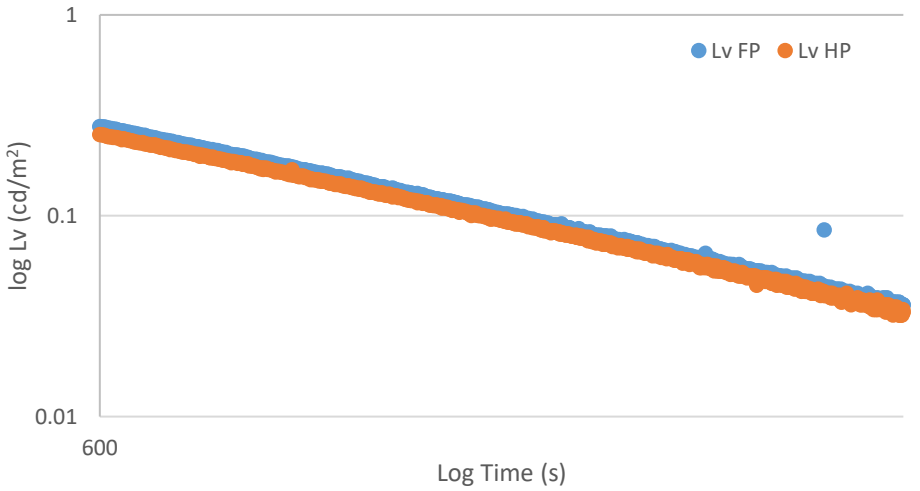

Figure 5-20. Log(L_v) vs. log(t) between 10 minutes to 60 minutes.

Results

The measured luminance (L_v) decay for "half power" and "full power" only differ significantly within the first 3 minutes as shown in Figure 5-19. After that the two begin to converge, as seen in Figure 5-20. These results support the field results that show little to no dependence on the amount of sunlight the installations received prior to sunset and give promise that even locations with overcast weather or low solar irradiance may be able to utilize photoluminesecnet stones effectively in concrete applications.

Driver's Perspective and Particle Attrition at the UF Installation

Duration and Intensity from a Driver's Perspective

As documented through time-lapse data collected overnight, the intensity of the light produced by the stones reaches peak values around 30 minutes after sunset. In order to visually qualify the brightness of the stones at night from the vantage-point of a possible driver, pictures were taken of the stones at this time from various perspectives and distances. Photographs of the sidewalk installation were taken at 6:03 pm on a day when the sun set at 5:33 pm. There are five photographs that display the installation from a south-west facing view (Figure 5-21through Figure 5-25) and five photographs that display the installation from a north-east facing view (Figure 5-26 through Figure 5-30). These sets of photographs are taken from points of reference up close to the installation, approximately 10 feet away, 20 feet away, 30 feet away, and 40 feet away in each respective orientation. Once the reference point was moved further than 40 feet away the light being emitted by the stones was visible but the design of the stones themselves became less visible due to the geometry of the sidewalk. In addition to these two main lines of orientation, Figure 5-33 displays the brightness of the stones from three more frames of reference. Overall, it is clear that the emitted light is easily detected by the human eye at night. This would lead to the conclusion that the application of aggregate similar spread would be beneficial to increase driver visibility at pedestrian/bicyclist pathways at night. The stones, however, do not appear to illuminate people or other objects that are near them.

Figure 5-21. Installation viewed from the southwest from close proximity 30 minutes after sunset.

Figure 5-22. Installation viewed from the southwest from 10 ft. 30 minutes after sunset.

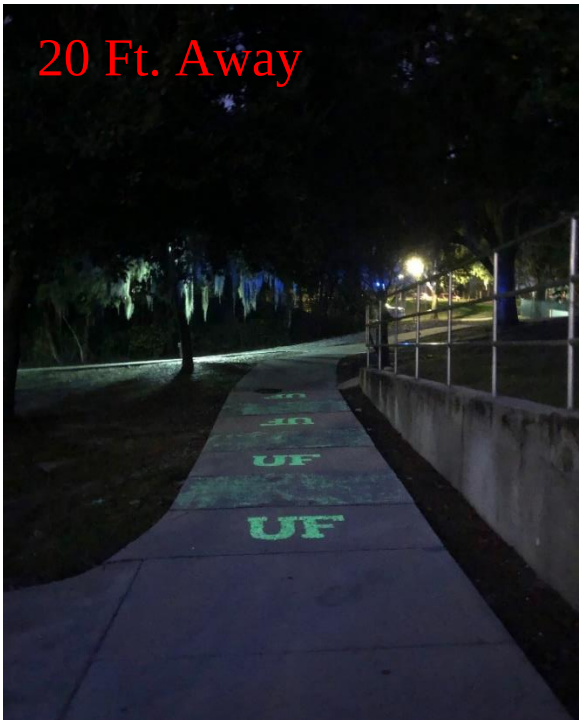

Figure 5-23. Installation viewed from the southwest from 20 ft. 30 minutes after sunset.

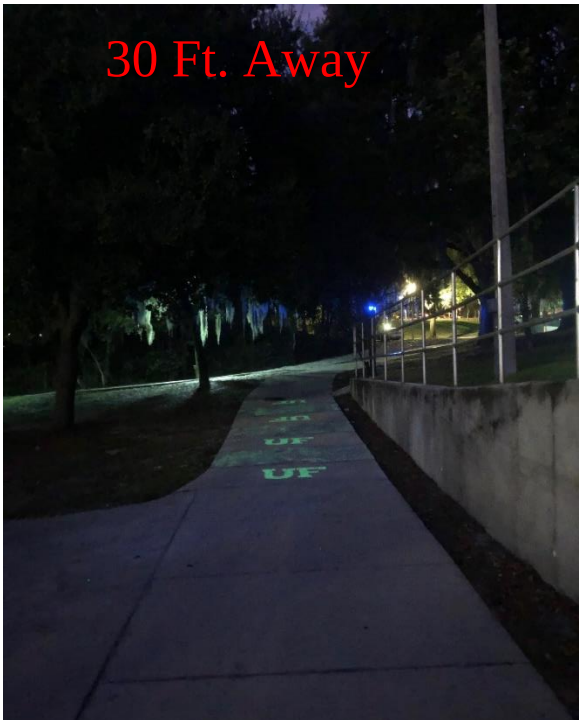

Figure 5-24. Installation viewed from the southwest from 10 ft. 30 minutes after sunset.

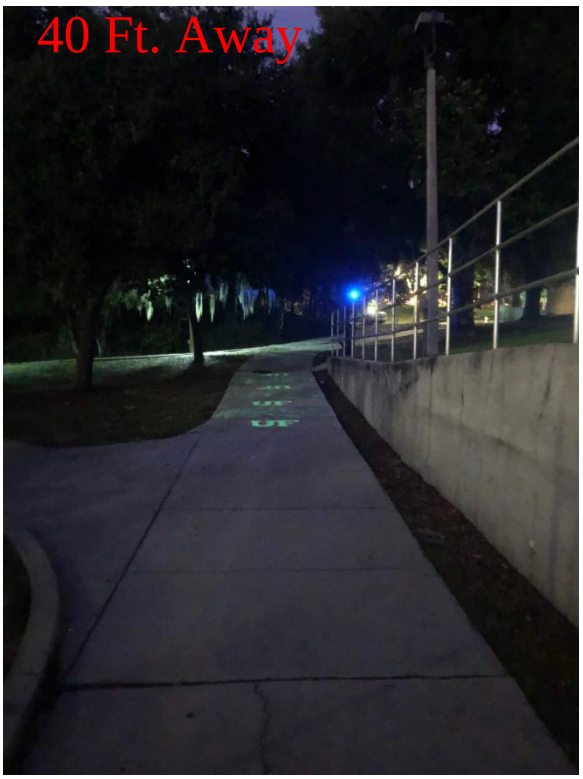

Figure 5-25. Installation viewed from the southwest from 40 ft. 30 minutes after sunset.

Figure 5-26. Installation viewed from the northeast at close proximity 30 minutes after sunset.

Figure 5-27. Installation viewed from northeast 10 ft. away 30 minutes after sunset.

Figure 5-28. Installation viewed from northeast 20 ft. away 30 minutes after sunset.

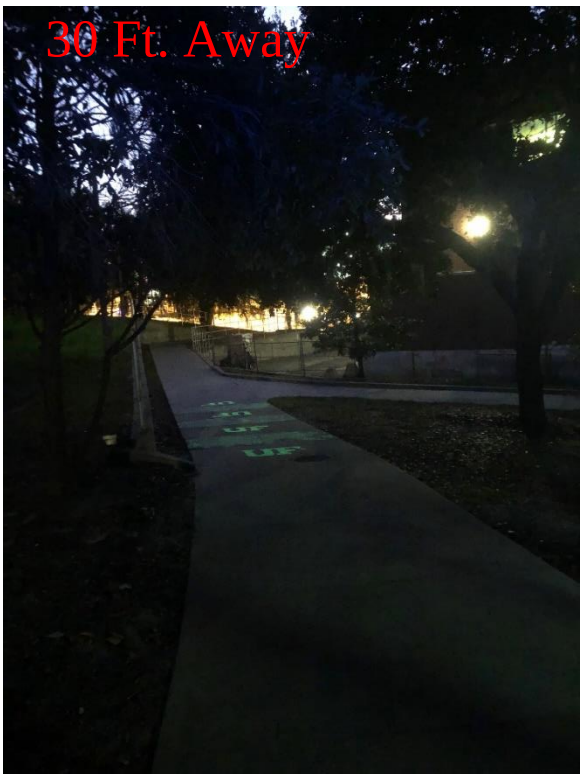

Figure 5-29. Installation viewed from northeast 30 ft. away 30 minutes after sunset.

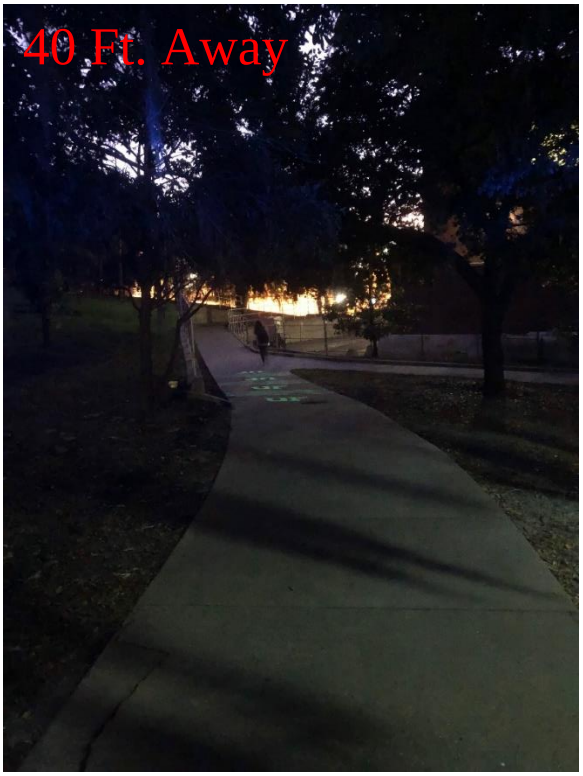

Figure 5-30. Installation viewed from northeast 40 ft. away 30 minutes after sunset.

Figure 5-31. Installation from an additional reference frame.

Figure 5-32. Installation from an additional reference frame.

Figure 5-33. Installation from an additional reference frame.

Figure 5-34. The last logo was placed after the concrete started to set, and some of the stones are coming loose.

Particle Attrition

For the most part the stones were well integrated into the concrete if they were placed soon after the concrete was poured. However, because the installation was time intensive (it took well over one hour with one student placing the stones and the contractor smoothing everything) using the stencils, the last couple of logos that were embedded are starting to show signs of attrition. This can be seen in Figure 5-34 below where stones are coming loose from the bottom portion of the logo. However, when the stones were placed sooner and then smoothed, they are well integrated and show no signs of attrition. An example of stones placed soon after pouring are shown in Figure 5-35. Here, the UF logo is perfectly intact. In sections where the stones were placed into the concrete using pre-fabricated sheets and then smoothed with a mechanical grinder, like that described in Figure 5-4, there were some signs of attrition, but this all occurred during the installation when the sheet cover was removed after curing and not over time. In fact, other than the small areas where particles were removed, these sections do not show any roughness or inhomogeneity like those used without grinding, as seen in Figure 5-37.

Figure 5-35. Stones that were placed while the concrete was still wet are showing no sign of attrition.

Figure 5-36. In this section of the installation, prefabricated sheets were used and then everything was sanded and ground down to make the surface smooth. In general, the glowing stones are all well integrated, but some were removed after the back covering was peeled away. Selected sections where stones are removed are indicated with the red circles.

Figure 5-37. A zoomed in look at one of the areas where stones were not well integrated.

References

1. Wattway. http://www.wattwaybycolas.com/en/
2. Modest, M. F., *Radiative heat transfer*. Academic Press: Radarweg 29, PO Box 211, 1000 AE Amsterdam, The Netherlands, 2013.
3. Roosegaarde, D. Factsheet Glowing Lines. 2015. https://www.studioroosegaarde.net/uploads/files/2014/11/13/205/Factsheet%20Van%20Gogh-Roosegaarde%20bicycle%20path.pdf
4. Anthony, S. World's first solar road opens in France: It's ridiculously expensive. 2016. http://arstechnica.com/cars/2016/12/worlds-first-solar-road-opens-in-france/
5. Lin, Y.; Tang, Z.; Zhang, Z., Preparation of long-afterglow $Sr_4Al_{14}O_{25}$-based luminescent material and its optical properties. *Materials Letters* **2001,** 51, (1), 14-18.
6. Matsuzawa, T.; Aoki, Y.; Takeuchi, N.; Murayama, Y., A New Long Phosphorescent Phosphor with High Brightness, $SrAl_2O_4:Eu^{2+}$, Dy^{3+}. *Journal of the Electrochemical Society* **1996,** 143, (8), 2670-2673.
7. Georgia Welcome Center on I-85 at Alabama Border Pioneers Solar Panels on Pavement. http://www.aashtojournal.org/Pages/122216gdot.aspx
8. Katsumata, T.; Sasajima, K.; Nabae, T.; Komuro, S.; Morikawa, T., Characteristics of Strontium Aluminate Crystals Used for Long-Duration Phosphors. *Journal of the American Ceramic Society* **1998,** 81, (2), 413-416.
9. Feldmann, C.; Jüstel, T.; Ronda, C. R.; Schmidt, P. J., Inorganic luminescent materials: 100 years of research and application. *Advanced Functional Materials* **2003,** 13, (7), 511-516.
10. Yamamoto, H.; Matsuzawa, T., Mechanism of long phosphorescence of $SrAl_2O_4:Eu^{2+}$, Dy^{3+} and $CaAl_2O_4$: Eu^{2+}, Nd^{3+}. *Journal of luminescence* **1997,** 72, 287-289.
11. Clabau, F.; Rocquefelte, X.; Jobic, S.; Deniard, P.; Whangbo, M. H.; Garcia, A.; Le Mercier, T., Mechanism of phosphorescence appropriate for the long-lasting phosphors Eu^{2+}-doped $SrAl_2O_4$ with codopants Dy^{3+} and B^{3+}. *Chemistry of Materials* **2005,** 17, (15), 3904-3912.
12. Källberg, S. *Measurement of photoluminescence according to DIN 67510-1:2009*; Smart Signs AS: Norway, 2011.
13. Jeon, G.-Y.; Hong, W.-H., An experimental study on how phosphorescent guidance equipment influences on evacuation in impaired visibility. *Journal of loss Prevention in the Process Industries* **2009,** 22, (6), 934-942.
14. Wong, W.-f. Development and applications of long afterglow luminescent materials. The Hong Kong Polytechnic University, Hong Kong, 2006.
15. Wang, L., Application of Long Afterglow Material in Highway Engineering. In *2015 2nd International Conference on Material Engineering and Application (ICMEA 2015)*, 2015.
16. Peters, A. Here's the First Glow-in-the-Dark Bike Lane in the U.S. https://transport.tamu.edu/about/news/2017/2017-02-fastcoexist-bikelane.aspx
17. Randall, J. T.; Wilkins, M. H. F., Phosphorescence and electron traps II. The interpretation of long-period phosphorescence. *Proceedings of the Royal Society of London. Series A. Mathematical and Physical Sciences* **1945,** 184, (999), 390-407.
18. Blasse, G.; Grabmaier, B. C., How Does a Luminescent Material Absorb Its Excitation Energy? In *Luminescent materials*, Springer: 1994; pp 10-32.
19. Ronda, C. R., *Luminescence: from theory to applications*. John Wiley & Sons: Federal Republic of Germany, 2007.
20. Schubert, E. F.; Cho, J.; Kim, J. K., Light-emitting diodes. *Kirk-Othmer Encyclopedia of Chemical Technology* **2000**, 1-20.

21. Walsh, J. W. T., *Photometry*. Constable & Company Ltd.: London, 1953.
22. Barbur, J. L.; Stockman, A., Photopic, mesopic and scotopic vision and changes in visual performance. *Encyclopedia of the Eye* **2010,** 3, 323-331.
23. Murphy Jr, T. W., Maximum spectral luminous efficacy of white light. *Journal of Applied Physics* **2012,** 111, (10), 104909.
24. Kaya, S. Y.; Karacaoglu, E.; Karasu, B., Effect of Al/Sr ratio on the luminescence properties of $SrAl_2O_4$: Eu^{2+}, Dy^{3+} phosphors. *Ceramics International* **2012,** 38, (5), 3701-3706.
25. Wong, W.-f., Development and applications of long afterglow luminescent materials. **2006**.
26. Alcón, N.; Tolosa, Á.; Picó, M.; Iñigo, I., A revision of the luminance decay time estimation methods for photoluminescent products. *Color Research & Application* **2011,** 36, (5), 383-389.
27. Florida, D. O. T., Standard specifications for road and bridge construction. *Florida Department of Transportation, Tallahassee, FL,* **2010**.
28. Wang, L.; Zhang, B.; Wang, D.; Yue, Z., Fundamental mechanics of asphalt compaction through FEM and DEM modeling. In *Analysis of asphalt pavement materials and systems: Engineering methods*, 2007; pp 45-63.